

# Nuclear beams in HERA

M.Arneodo<sup>a</sup>, A.Bialas<sup>b</sup>, M.W.Krasny<sup>c</sup>, T.Sloan<sup>d</sup> and M. Strikman<sup>e</sup>

<sup>a</sup> Università di Torino, I-10125 and INFN Cosenza, Italy

<sup>b</sup> Institute of Physics, Jagellonian University, Cracow, Poland

<sup>c</sup> LPNHE, Universités Paris VI and VII, IN2P3-CNRS, Paris, France

<sup>d</sup> School of Physics and Chemistry, University of Lancaster, Lancaster LA1 4YB, UK

<sup>e</sup> Pennsylvania State University, University Park, PA 16802, USA

**Abstract:** A study has been made of the physics interest and feasibility of experiments with nuclear beams in HERA. It is shown that such experiments widen considerably the horizon for probing QCD compared to that from free nucleon targets. In addition there is some sensitivity to physics beyond the standard model. Hence the option to include circulating nuclear beams in HERA allows a wide range of physics processes to be studied and understood.

(Submitted to the Proceedings of the Workshop on Future Physics at HERA)

## 1 Introduction

The successes of QCD in describing *inclusive* perturbative phenomena have moved the focus of investigations to new frontiers. Three fundamental questions to be resolved are the space-time structure of high-energy strong interactions, the QCD dynamics in the nonlinear, small coupling domain and the QCD dynamics of interactions of fast, compact colour singlet systems.

The study of electron-nucleus scattering at HERA allows a new regime to be probed experimentally for the first time. This is the regime in which the virtual photon interacts coherently with all the nucleons at a given impact parameter. In the rest frame of the nucleus this can be visualized in terms of the propagation of a small  $q\bar{q}$  pair in high density gluon fields over much larger distances than is possible with free nucleons. In the Breit frame it corresponds to the fact that small  $x$  partons cannot be localized longitudinally to better than the size of the nucleus. Thus low  $x$  partons from different nucleons overlap spatially creating much larger parton densities than in the free nucleon case. This leads to **a large amplification of the nonlinear effects expected in QCD at small  $x$** . The HERA  $ep$  data have confirmed the rapid increase of the parton densities in the small  $x$  limit predicted by perturbative QCD. However the limited  $x$  range available at HERA makes it difficult to distinguish between the predictions of the DGLAP evolution equations and the BFKL-type dynamics. Moreover, the nonlinear effects expected at small  $x$  are relatively small in  $ep$  scattering in the HERA kinematic domain and it may be necessary to reduce  $x$  by at least one order of magnitude to observe unambiguously

such effects. However, the amplification obtained with heavy nuclear targets **allows an effective reduction of about two orders of magnitude in  $x$**  making it feasible to explore such nonlinear effects at the energies available at HERA. The question of nonlinear effects is one of the most fundamental in QCD. It is crucial for understanding the kind of dynamics which would slow down and eventually stop the rapid growth of the cross section (or the structure function,  $F_2$ ) at small  $x$ . It is also essential in order to understand down to what values of  $x$  the decomposition of the cross section into terms with different powers of  $\frac{1}{Q^2}$  remains effective. It is important for the understanding of the relationship between hard and soft physics. One can also study the dynamics of QCD at high densities and at zero temperatures raising questions complementary to those addressed in the search for a quark-gluon plasma in high-energy heavy ion collisions.

Deep inelastic scattering from nuclei provides also a number of ways to probe **the dynamics of high-energy interactions of small colour singlet systems**. This issue started from the work of Gribov [1] who demonstrated the following paradox. If one makes the natural (in soft physics) assumption that at high energies any hadron interacts with a heavy nucleus with cross section  $2\pi R_A^2$  (corresponding to interaction with a black body), Bjorken scaling at small  $x$  is grossly violated –  $\sigma_{\gamma^*A} \propto \ln Q^2$  instead of  $\frac{1}{Q^2}$ . To preserve scaling, Bjorken suggested, using parton model arguments, that only configurations with small  $p_t \leq p_{t0}$  are involved in the interaction (the Aligned Jet Model) [2]. However, in perturbative QCD Bjorken’s assumption does not hold – large  $p_t$  configurations interact with finite though small cross sections (colour screening), which however increase rapidly with incident energy due to the increase of the gluon density with decreasing  $x$ . Hence again one is faced with a fundamental question which can only be answered experimentally: *Can small colour singlets interact with hadrons with cross sections comparable to that of normal hadrons?* At HERA one can both establish the  $x, Q^2$  range where the cross section of small colour singlets is small – *colour transparency*, and look for the onset of the new regime of large cross sections, *perturbative colour opacity*.

Another fundamental question to be addressed is **the propagation of quarks through nuclear matter**. At large energies perturbative QCD leads to the analogue of the Landau-Migdal-Pomeranchuk effect in quantum electrodynamics. In particular Baier et al. [3] find a highly nontrivial dependence of the energy loss on the distance,  $L$ , travelled by a parton in a nuclear medium: the loss instead of being  $\propto L$  is  $\propto L^2$ . Several manifestations of this phenomenon can be studied at HERA.

There is also an *important connection to heavy ion physics*. Study of  $eA$  scattering at HERA would be important for the analysis of heavy ion collisions at the LHC and RHIC. Measurements of gluon shadowing at small  $x$  are necessary for a reliable interpretation of the high  $p_t$  jet rates at the LHC. In addition, the study of parton propagation in nuclear media is important for the analysis of jet quenching phenomena, which may be one of the most direct global signals of the formation of a quark-gluon plasma.

Current fixed target data on lepton-nucleus scattering only touch the surface of all these effects due to the limited  $Q^2$  range of the data at small  $x$ . Indeed the  $Q^2$  range of these data is too small to distinguish the contribution of the vector meson dominance behaviour of the photon from its hard QCD behaviour at small  $x$ . The range of  $x$  and  $Q^2$  in experiments with nuclei at HERA compared to the fixed target experiments is shown in Fig. 1. It can be seen that at HERA the kinematic range will be extended well into the deep inelastic scattering region.

To address the questions discussed above we identify the primary experimental programme for nuclei in HERA as:

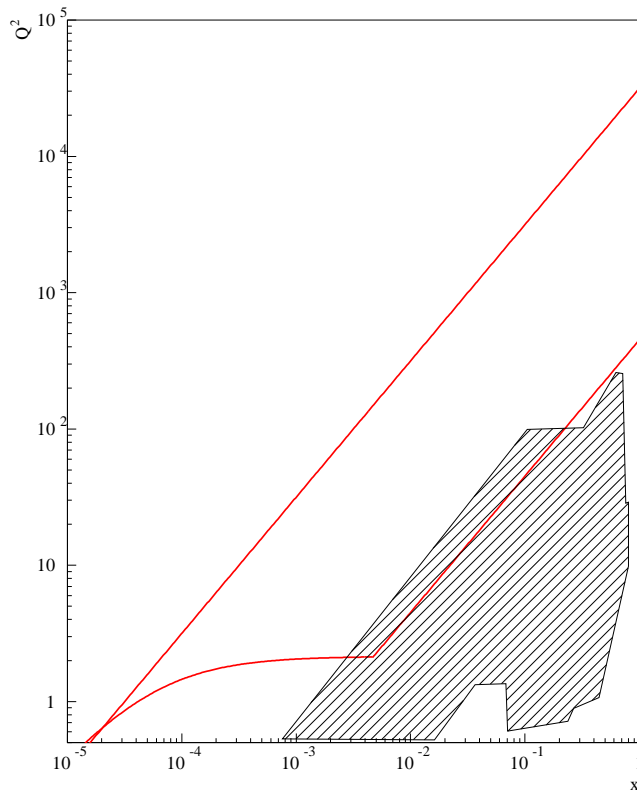


Figure 1: The kinematic region covered by experiments at HERA compared to fixed target data (shaded region).

- **Study of the  $x$  and  $Q^2$  dependence of nuclear shadowing over a wide  $Q^2$  range.** This will allow the processes limiting the growth of  $F_2$  as  $x$  tends to zero to be studied in detail.
- **To establish the difference between the gluon distributions of bound and free nucleons.** This will allow the part played by gluon fusion in the shadowing process to be studied directly.
- **Study of diffractive processes:** to see if the pomeron generated by nuclei shows any difference from that generated by free nucleons. Processes such as vector meson production can also be used to search for colour transparency.
- **Study of hadronic final states.** This allows the propagation of partons in the nuclear medium to be studied as well as the multiplicity fluctuations discussed later.

The proceedings of Working Group 8 are organised as follows. First we give an experimental overview in which we demonstrate the feasibility of carrying out this experimental programme. Then we give a theoretical overview in which we explain the relevance of the programme to QCD. Finally, we give the detailed contributions on different topics which demonstrate the depth of the physics interest. The proposed measurements in the main will be possible with the existing detectors H1 and ZEUS measuring down to low  $Q^2$  and with luminosities at the level of 1-10  $\text{pb}^{-1}$  per nucleon. The contribution of Chwastowski and Krasny [4] shows that if the detectors could extend their rapidity coverages various experiments of interest to nuclear structure physicists become feasible.

## 2 Experimental Overview

## 2.1 Introduction

In the following subsections the feasibility of the measurements defined above as the primary experimental programme is investigated. The nuclear targets should each have  $Z/A$  of  $1/2$ . Hence the energy of each nucleon in a deep inelastic collision will be half that of the HERA proton energy of 820 GeV i.e. 410 GeV. The electron energy is assumed to have the standard value of 27.6 GeV. We show that most studies can be carried out with the existing detectors requiring luminosities between  $1\text{-}10\text{ pb}^{-1}$  per nucleon. While the possibility of storing heavy nuclei up to Sn and Pb is very attractive, a program covering the light isoscalar nuclei (D,  $^4\text{He}$ , C, S) would by itself have a major discovery potential. The necessary radiative corrections are described in the contributions of Kurek [5] and of Akushevich and Spiesberger [6] who show that such corrections can be kept under control using suitable cuts on the data. In most of the experiments it is proposed to measure ratios of yields. Hence, in order to minimise systematic errors, it is desirable to store different nuclei in HERA simultaneously. Otherwise frequent changes of the stored nucleus in the beam will be necessary.

## 2.2 Shadowing Measurements Using Nuclei in HERA

The accuracy of shadowing measurements for an experiment in which nuclear targets are stored in HERA is calculated. It is shown that for luminosities of  $2\text{ pb}^{-1}$  per nucleon the measurements would extend considerably the accuracy and range of the existing data.

The  $x$  dependence of the differences in the nucleon structure function between bound and free nucleons has been well measured in recent years in fixed target experiments [7, 8, 9, 10, 11] following the discovery of the differences in the 1980s [12, 13, 14, 15, 16]. The present experimental situation on this  $x$  dependence is briefly summarised in Fig. 2. However, the  $Q^2$  dependence is not well measured. In the shadowing region the data are at such low  $Q^2$  values that they are arguably not even in the deep inelastic regime.

There are many different models [17] for the effects in the different regions shown in Fig. 2 which are all compatible with the existing data. In the shadowing region the  $Q^2$  range of the data is insufficient to separate the different contributions from the vector dominance behaviour of the photon and QCD effects such as parton fusion. Measurements over the extended  $x$  and  $Q^2$  ranges, which would become possible at HERA, will give more information to help separate the models and help us understand the phenomena which limit the rise of the nucleon structure function  $F_2$  at small  $x$ ; e.g. see references [18, 19].

### Is it feasible to study shadowing in HERA?

To answer this question we assume that nuclear beams can be stored in HERA and luminosities of  $2\text{ pb}^{-1}$  per nucleon, shared between 2 nuclear targets, can be achieved (i.e.  $2/A\text{ pb}^{-1}$  per nucleus, where  $A$  is the atomic weight). With this definition of luminosity, rate computations should use cross sections per nucleon. The counting rates in bins of  $Q^2$  and  $x$  are then estimated to assess the statistical errors on the measurements of the ratios of  $F_2^A/F_2^D$  where the nuclear targets are assumed to be He, C or S. The cross sections are calculated from the one photon exchange formula

$$\frac{d^2\sigma}{dx dQ^2} = \frac{4\pi\alpha^2}{xQ^4} \left[ 1 - y + \frac{y^2}{2(1+R)} \right] F_2(x, Q^2). \quad (1)$$

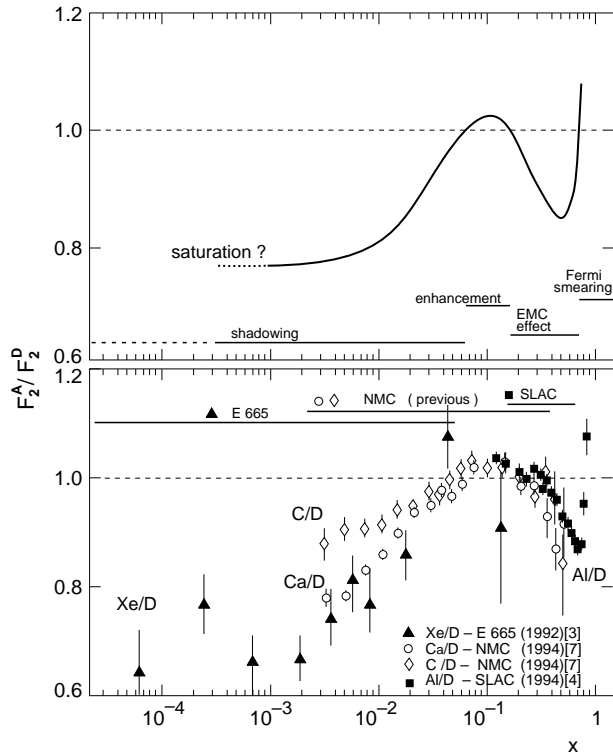


Figure 2: Partial compilation of results for  $F_2^A/F_2^D$  (from [8]). Note that below  $x \approx 0.01$ , the average  $Q^2$  value of the data is smaller than  $2 \text{ GeV}^2$ .

The nucleon structure functions,  $F_2$  and  $R$ , are computed from the MRS(A) set [20]. Deep inelastic scattering events are assumed to be detectable with 100% efficiency if the scattered electron energy  $E' > 5 \text{ GeV}$  and its scattering angle is more than 3 degrees to the electron beam. Alternatively events are assumed to be detectable with 100% efficiency if a quark is scattered out by an angle of more than 10 degrees to the proton beam and with an energy more than  $5 \text{ GeV}$ . Nuclear effects on the structure functions are neglected. Such effects, which are at the 10% level, will have little effect on the statistical accuracy of measurements of ratios of structure functions,  $F_2^A/F_2^D$ .

Fig. 3 shows the estimated statistical errors on the ratios (averaged over  $Q^2$ ), with these assumptions, together with the measurements of the NMC [8]. In many cases the statistical errors are  $< 1\%$  i.e. smaller than the sizes of the points. It can be seen from Fig. 3 that this statistical precision will allow high accuracy measurements of the shadowing ratios down to lower  $x$  values than in fixed target experiments and over a much wider range of  $Q^2$ .

Fig. 4 shows the statistical precision of the slopes  $d(F_2^A/F_2^D)/d \ln Q^2$  estimated at HERA compared to the NMC data. Impressive precision is possible at HERA, presumably due to the much larger  $Q^2$  range covered. Measurements over such a large  $Q^2$  range will allow the precise predictions of the parton fusion model to be tested.

If at least two different nuclear targets can be stored in different bunches in HERA during experimental running the systematic errors should be similar in magnitude to those in fixed target experiments [7]. Radiative corrections for deep inelastic scattering from heavy nuclear targets will be necessary and these will be applied with the appropriate cuts on the data as discussed in these proceedings [5, 6].

In conclusion, measurements of the ratios ( $F_2^A/F_2^D$ ) at HERA will extend the data to smaller values of  $x$  and much larger values of  $Q^2$  than in fixed target experiments. Impressive precision on the  $Q^2$  dependence will be possible from which the mechanism which leads to the limitation in the rise of  $F_2$  at small  $x$  and large  $Q^2$  can be studied.

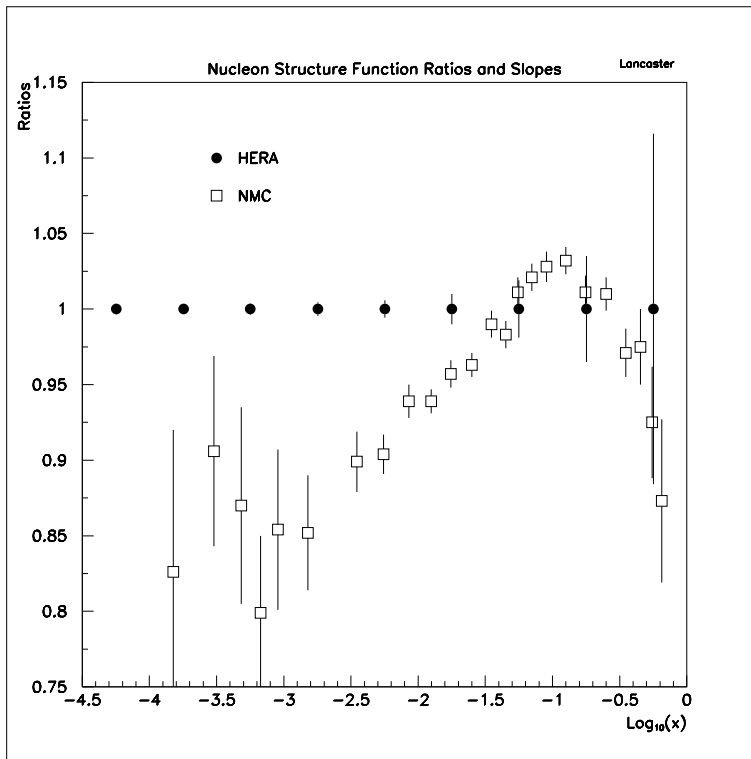


Figure 3: Ratio of the nucleon structure function in carbon to that in deuterium as a function of  $x$ . The NMC data [8] (open squares) are shown in comparison to data with the estimated statistical accuracy of an experiment of luminosity  $1 \text{ pb}^{-1}$  per nucleon at HERA.

## 2.3 The Accuracy of The Gluon Density Measurements Using Nuclei in HERA

### 2.3.1 Introduction

The major contribution to shadowing from nonlinear QCD effects is thought to arise from multigluon interactions such as gluon fusion effects. Such effects are amplified at higher  $x$  in nuclei due to the larger target size so that they should become visible in the HERA kinematic range. Similar effects are expected to limit the growth of the nucleon structure function  $F_2$  at high  $Q^2$  and low  $x$ . Hence it is interesting to look for such effects directly on the gluon distribution by looking for differences between the gluon density in bound and free nucleons. Different ways of doing this are studied below.

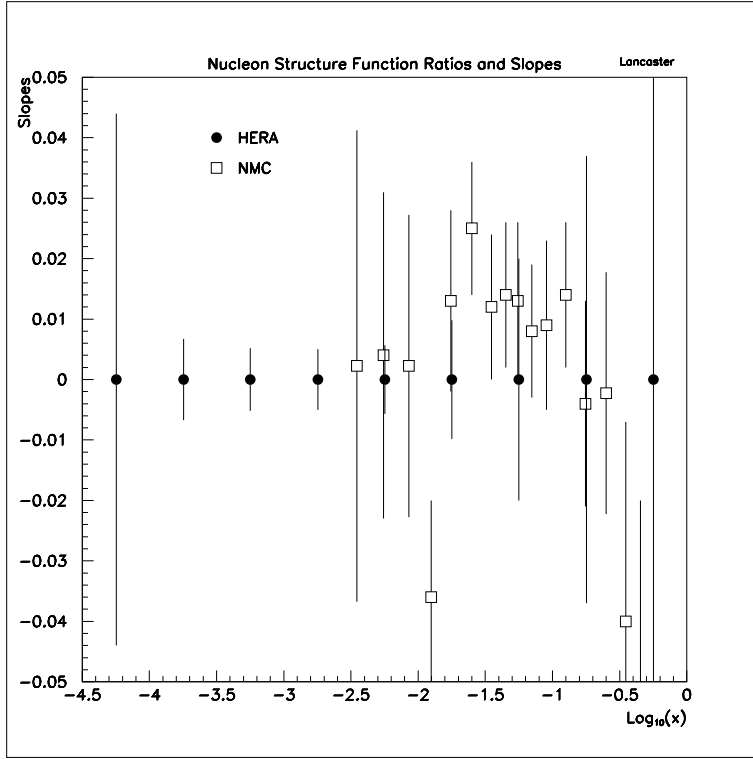


Figure 4: The slopes  $d(F_2^A/F_2^D)/d\ln Q^2$  as function of  $x$  showing the NMC data [7] (open squares) and the statistical accuracy of an experiment with  $1 \text{ pb}^{-1}$  per nucleon at HERA.

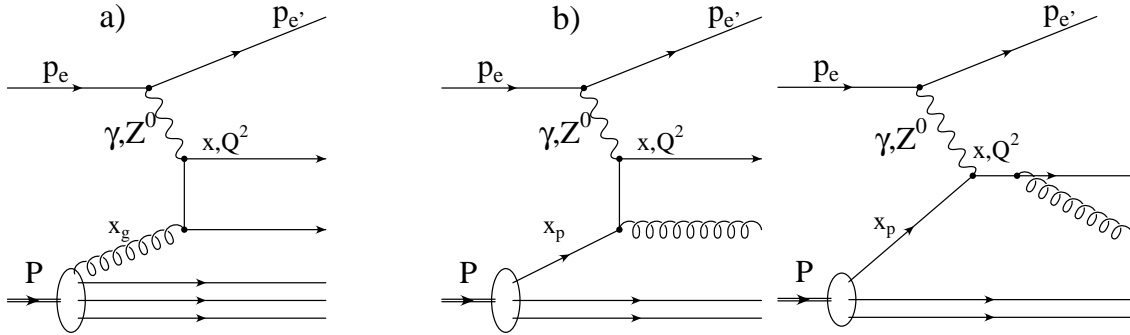


Figure 5: The processes giving rise to 2 + 1 jet topology. P denotes here the projectile particle, a proton or a nucleus,  $Q^2$  is the four-momentum transfer and  $x$  is the Bjorken variable.

### 2.3.2 Determination of the Gluon Density in the Nucleus from the Jet Rates

In the majority of large  $Q^2$  deep inelastic electron-nucleus scattering events, at HERA, the scattered quark and the remnant of the nucleus will hadronize to form two jets. Such a topology is often called the 1 + 1 jet configuration. Occasionally, however, more jets will be produced. In Fig. 5 the partonic processes giving rise to the 2 + 1 jet topology are shown. These processes are called “boson-gluon fusion” (process a) and “the QCD Compton scattering” (processes b).

The 2 + 1 jet events can be related to the partonic processes shown in Fig. 5 if the invariant

mass of the system of two jets  $\bar{s} = (p_{jet1} + p_{jet2})^2$  is significantly larger than the typical scale of the strong interactions, so that perturbative QCD can be used. The contribution of these processes to the total cross section depends upon the value of the coupling constant  $\alpha_s$  defining the strength of quark-gluon coupling and upon the momentum distribution of the incoming gluon (quark). The fractions of the parent bound nucleon momentum carried by the incoming partons,  $x_{p,g}$ , are constrained by the value of  $x$ , the total hadronic mass,  $W$ , and the invariant mass of the two jet system  $\bar{s}$ :

$$x_{p,g} = x + \bar{s}/W^2. \quad (2)$$

For values of  $\bar{s}/W^2 \geq 0.01$ , the values of  $x_{p,g}$  must be large. In this kinematic domain the partonic distributions in bound nucleons have been well measured in fixed target experiments [17]. Thus, the coupling constant,  $\alpha_s$ , can be derived from the measured rate of 2 + 1 jet events. In turn, we shall be able to use this  $\alpha_s$  value to determine the gluon momentum distribution at smaller  $x_g$ , corresponding to small values of both  $x$  and  $\bar{s}/W^2$  (note that at small  $x$  the contribution of the QCD Compton processes (Fig. 5b,c) to the total “2+1” jet cross section is expected to be small). Such an analysis has been recently carried out by the H1 collaboration [21] using deep inelastic electron-proton scattering data collected at HERA. The systematic errors of the resulting gluon density are large and to some extent uncertain. They are dominated by the uncertainties in relating the measured rate of observed jet topologies to the basic QCD processes involving quarks and gluons. Unfolding the gluon densities involves modelling the hadronisation of the quarks which is necessary for simulating the detector effects but is only weakly constrained by the data. In addition several jet algorithms can be used leading to differences in jet counting. There exist as well ambiguities in the QCD calculation of the processes shown in Fig. 5. The amplitudes of the processes  $\gamma^*g \rightarrow jet_1 + jet_2$  and  $\gamma^*q \rightarrow jet_1 + jet_2$  have poles corresponding to the collinear emission of jets with respect to the direction of the incoming gluon ( $\gamma^*$ ) and to the emission of jets of small invariant mass. Since one must use fixed order perturbative QCD, jets reconstructed in phase space close to the poles must be avoided to diminish the sensitivity to higher order terms which have so far not been calculated. This can be achieved by using only jets of high invariant mass ( $\bar{s} \geq 100 \text{ GeV}^2$ ) and by rejecting events in which one of the jets is emitted at a small angle with respect to the incoming proton direction. In the region of small  $\bar{s}$  the jet rates calculated using leading order and next to leading order approximations are significantly different [22] indicating that higher order corrections are necessary for an unambiguous determination of the gluon density.

Will it be possible to use the jet method to determine the gluon density in nuclei given the uncertainties described above and at the same time adding the extra ambiguity related to jet formation in the nuclear medium? Most likely it will be difficult to obtain satisfactory precision in measuring the absolute gluon distributions in the nuclei. However, we expect that good precision can be achieved in measuring the ratios of gluon distributions for various nuclei. The uncertainties due to the jet finding algorithms and to the modelling of the hadronisation processes will largely cancel in the ratios if high energy jets are used. High energy jets are expected to be formed outside the nucleus. In addition we shall be able to select jets in the restricted phase space region where the effects of rescattering of slow particles belonging to the jet but formed inside the nucleus are small. The energy loss of quarks and gluons traversing the nuclear medium prior to hadronisation is expected to be below 350 MeV/fm according to the estimation of [3] and should not give rise to large errors on the gluon density ratio. The expected statistical precision of the measurements of the ratio of the gluon densities for two nuclei of atomic numbers A1 and A2 is shown in Fig. 6. It corresponds to a luminosity of 10



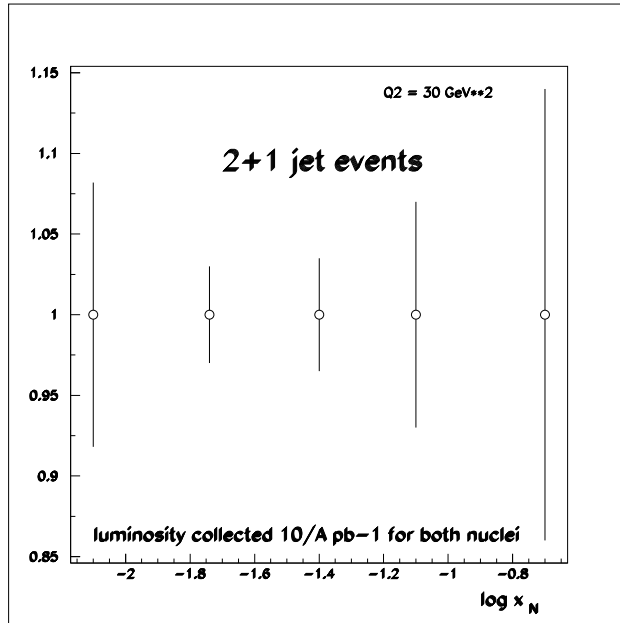


Figure 6: Statistical precision of the ratio of gluon densities in two nuclei  $x_N G(x_N, A_1)/xG(x_N, A_2)$  at  $Q^2 = 30 \text{ GeV}^2$  determined from the “2 + 1” jet sample.

$\text{pb}^{-1}/A$  for each nucleus. In estimating this statistical precision we have followed the jet and kinematic region selection of [21] and neglected all nuclear effects. We also assume that the contribution of the QCD Compton process can be unambiguously subtracted. The  $x_N$  variable is the fraction of the bound nucleon momentum carried by the gluon. It is clear that good statistical precision on the measurement of the ratio of the gluon densities can be achieved at modest luminosities.

### 2.3.3 The Gluon Distribution in Nuclei from Scaling Violations

The gluon distribution can also be determined from the deviations from scaling of the structure function  $F_2$ . We estimate the accuracy of such a determination of the gluon density for bound nucleons in an experiment with nuclear beams in HERA. The scaling violations of  $F_2$  are strongly related to the gluon distribution of the target nucleon at small  $x$  values. The quantity

$$\psi = \frac{\frac{dF_2^A}{d\ln Q^2} - \frac{dF_2^D}{d\ln Q^2}}{\frac{dF_2^p}{d\ln Q^2}} \quad (3)$$

is sensitive to the differences of the gluon distribution in bound and free nucleons and is roughly proportional to  $\delta G/G$  where  $G$  is the gluon density at a particular  $x$  value and  $\delta G$  is the difference in gluon densities between bound and free nucleons. Hence it would be interesting to measure this quantity in an experiment with nuclear beams stored in HERA.

To estimate the feasibility of such a measurement the accuracies of the determinations of the slopes  $dF_2/d\ln Q^2$  have been estimated from the expected counting rates for a  $2 \text{ pb}^{-1}$  per nucleon run using the MRS(A) set of structure functions [20]. The slopes were obtained from a linear least squares fit to values of  $F_2$  using the statistical errors calculated for such an experiment with the assumptions described in section 2.2. The error in the quantity  $\psi$  was then obtained assuming equal statistical errors for the nuclear and deuteron targets with a  $1 \text{ pb}^{-1}$  per nucleon run for each. The error on the slope  $dF_2^p/d\ln Q^2$  for the proton was neglected since this should be well determined from high luminosity proton running.

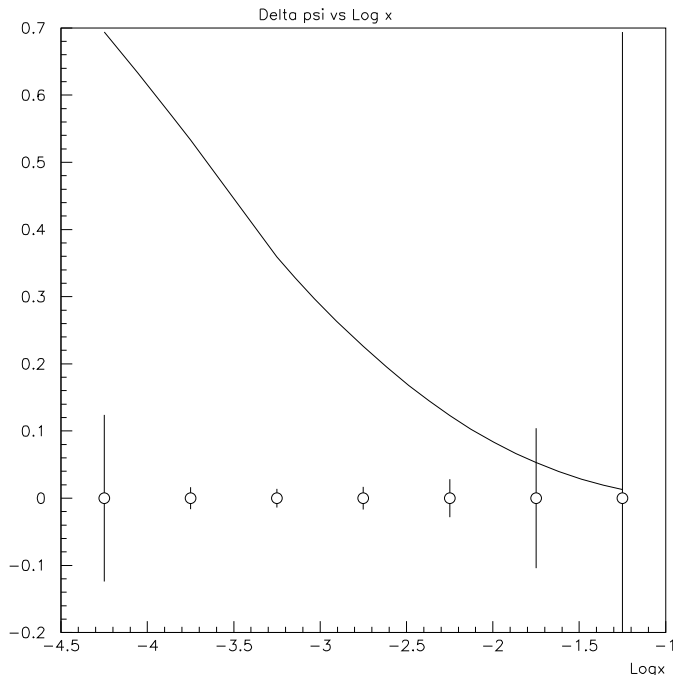


Figure 7: Accuracy of the difference between the slopes of  $F_2$  between nuclei and deuterium as a function of  $x$ . The smooth curve shows the calculated slope for the free proton.

The results are shown in Fig. 7. For the purpose of this figure we assume that the gluon densities for bound and free nucleons are the same so that  $\psi=0$ . The estimated statistical errors are then superimposed on these values and the smooth curve shows  $dF_2^p/d \ln Q^2$  for comparison computed from the MRS(A) set. Comparison of the errors on  $\psi$  with the values of the slope for the proton shows that this method will be sensitive to differences in the gluon densities between bound and free nucleons of the order of 5 per cent of the total gluon density at  $x$  in the vicinity of  $10^{-3}$ . Hence the measurement will be quite sensitive to nuclear effects on the gluon density.

### 2.3.4 Determination of the Gluon Density in the Nucleus from Inelastic $J/\psi$ production

The expected accuracy of the determination of the bound to free nucleon gluon density ratio  $xG|_A/xG|_D$  using nuclei in HERA is estimated for inelastic photoproduction of  $J/\psi$  mesons at  $Q^2 < 4 \text{ GeV}^2$  ( $eA \rightarrow eXJ/\psi$ ).

Inelastic production of  $J/\psi$  mesons has been used for a long time to extract or constrain the gluon distribution in the nucleon (see e.g. [23]-[28]), assuming that the dominant mechanism is the photon-gluon fusion [29]-[32]. Within this framework, the cross section is directly proportional to the gluon density. These calculations have been affected in the past by large normalisation uncertainties (up to factors of 2-5), which however have been greatly reduced recently [33]. Inelastic  $J/\psi$  production dominates at values of  $z$ , the fraction of the photon energy carried by the meson in the nucleon rest frame, smaller than  $\approx 0.9$ . In the framework of the colour singlet model [32], the gluon distribution is probed at a value of  $x$ , the fraction of the proton's momentum carried by the gluon,  $x = [m_{J/\psi}^2/z + p_t^2/z(1-z)]/W^2$ , where  $p_t$  is the  $J/\psi$  transverse momentum with respect to the virtual photon direction and  $W$  is the photon-nucleon centre-of-mass energy. The scale probed by this process is approximately  $m_{J/\psi}^2 \approx 10 \text{ GeV}^2$ .

Fig. 8 shows the expected statistical accuracy as a function of  $\log_{10} x$  for an integrated luminosity of  $10 \text{ pb}^{-1}/A$ . Decays into  $e^+e^-$  or  $\mu^+\mu^-$  pairs have been assumed. The plot refers to the kinematic region  $Q^2 < 4 \text{ GeV}^2$ ,  $z < 0.9$ . Nuclear effects have been neglected in the evaluation of statistical accuracies.

Possible sources of systematic uncertainties are the luminosity, the branching ratio, the global acceptance (including trigger and reconstruction efficiency, muon or electron identification etc.), the feed-in from  $\psi'$  production and the contamination from resolved photon events. In the recent H1 [26] and ZEUS [27] analyses, the total systematic uncertainty is approximately 10-20%. By and large all the above contributions would cancel in a ratio for simultaneously stored nuclei, with the partial exception of the luminosity. In practice, for an integrated luminosity of  $10 \text{ pb}^{-1}$ , the statistical uncertainty dominates.

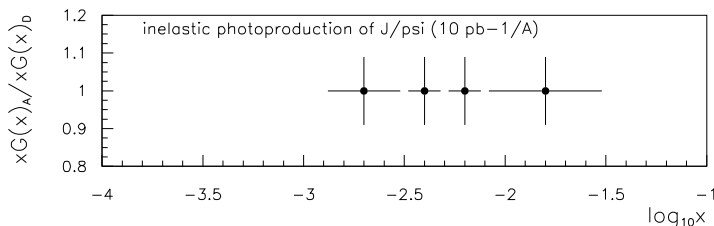


Figure 8: Expected statistical accuracy (vertical error bars) on the ratio  $xG|_A/xG|_D$  as a function of  $\log_{10} x$  using inelastic photoproduction ( $Q^2 < 4 \text{ GeV}^2$ ) of  $J/\psi$  mesons. An integrated luminosity of  $10 \text{ pb}^{-1}/A$  for each nucleus has been assumed. The horizontal bars indicate the size of the bins.

## 2.4 Diffraction from Nuclei in HERA

### 2.4.1 Introduction

The measurements of the ZEUS and H1 collaborations [34, 35] of deep-inelastic electron-proton scattering have revealed the existence of a distinct class of events in which there is no hadronic energy flow in an interval of pseudo-rapidity,  $\eta$ , adjacent to the proton beam direction i.e. events with a large rapidity gap. Such events are interpreted as deep inelastic scattering from the pomeron,  $P$ . Studies of events with a large rapidity gap from nuclear targets will allow the structure of the pomeron from a different source than the free nucleon to be determined. It will be interesting to see if these structures differ. In addition, the study of diffractive vector meson production will be interesting to search for the phenomenon of colour transparency. Such a phenomenon has not yet been convincingly seen although it is predicted in QCD.

### 2.4.2 Expected Accuracy of the Measurements of the Pomeron Structure

We commence by describing the terminology surrounding measurements of the Pomeron structure. In our studies we shall use the four variables  $\beta_A$ ,  $Q^2$ ,  $x_A$  and  $t_A$ , or equivalently  $\beta_A$ ,  $Q^2$ ,  $x_{P,A}$  and  $t_A$ , which are defined as follows:

$$x_A = \frac{-q^2}{2P \cdot q}; \quad x_{P,A} = \frac{q \cdot (P - P')}{q \cdot P}; \quad Q^2 = -q^2; \quad \beta_A = \frac{-q^2}{2q \cdot (P - P')}; \quad t_A = (P - P')^2. \quad (4)$$

Here  $q$ ,  $P$  and  $P'$  are, as indicated in Fig. 9, the 4-momenta of the virtual boson, incident nucleus and the final state colourless remnant  $Y$  respectively. The latter can be either a coherently recoiling nucleus or any incoherent excitation of the nucleus carrying its quantum numbers. The variables in equation (4) are related to each other via the expression:

$$x_A = \beta_A x_{P,A}. \quad (5)$$

We also introduce, in order to allow the comparison of measurements with nuclei of different atomic number  $A$ , the variables:

$$x = x_A \cdot A \quad x_P = x_{P,A} \cdot A \quad \beta = \beta_A \quad t = t_A. \quad (6)$$

Note that relation (5) rewritten in terms of the above variables still holds i.e.

$$x = \beta x_P. \quad (7)$$

The  $A$ -rescaled variables can be directly related to the variables defined in [36, 37] retaining their interpretation, as was given there, for processes in which only one nucleon of the nucleus interacts with the electron and the nucleon's Fermi momentum can be neglected.

The variables  $x_{P,A}$ ,  $x_P$  and  $\beta$  can be expressed in terms of the invariant mass of the hadronic system  $X$ ,  $M_X$ , the nucleus mass,  $M_A$ , and the total hadronic invariant mass  $W$  as

$$x_{P,A} = \frac{Q^2 + M_X^2 - t}{Q^2 + W^2 - M_A^2} \approx \frac{Q^2 + M_X^2}{Q^2} \cdot x_A, \quad (8)$$

$$x_P \approx \frac{Q^2 + M_X^2}{Q^2} \cdot x, \quad (9)$$

$$\beta = \beta_A = \frac{Q^2}{Q^2 + M_X^2 - t} \approx \frac{Q^2}{Q^2 + M_X^2}. \quad (10)$$

In the kinematic domain which we shall consider here ( $M_A^2 \ll W^2$  and  $|t| \ll Q^2$ ,  $|t| \ll M_X^2$ )  $x_{P,A}$  may be interpreted as the fraction of the 4-momentum of the nucleus carried by the  $P$  and  $\beta$  as the fraction of the 4-momentum of the  $P$  carried by the quark interacting with the virtual boson. Note that in the interactions in which only one nucleon takes part,  $x_P$  can be interpreted as the fraction of the 4-momentum of this nucleon carried by the  $P$ .

We shall follow in our analysis the formalism defined in [36, 37] and introduce the diffractive structure function  $F_{2,A}^{D(3)}$  as a function of three kinematic variables, derived from the structure function  $F_{2,A}^{D(4)}$ . This latter structure function depends upon four kinematic variables chosen here as:  $x$ ,  $Q^2$ ,  $x_P$  and  $t$  and is defined by analogy with the decomposition of the unpolarised total  $eA$  cross section. The total cross section can be expressed in terms of two structure functions  $F_{2,A}^{D(4)}$  and  $\frac{F_{2,A}^{D(4)}}{2x(1+R_A^{D(4)})}$  in the form

$$\frac{d^4\sigma_{eA \rightarrow eXY}}{dx dQ^2 dx_P dt} = A \cdot \frac{4\pi\alpha^2}{xQ^4} \left\{ 1 - y + \frac{y^2}{2[1 + R_A^{D(4)}(\beta, Q^2, x_P, t)]} \right\} F_{2,A}^{D(4)}(\beta, Q^2, x_P, t), \quad (11)$$

in which  $y = Q^2/sx_A$  and  $s$  is the  $eA$  collision centre of mass (CM) energy squared. We shall discuss here the low  $y$  region and neglect the term containing  $R_A^{D(4)}$ .

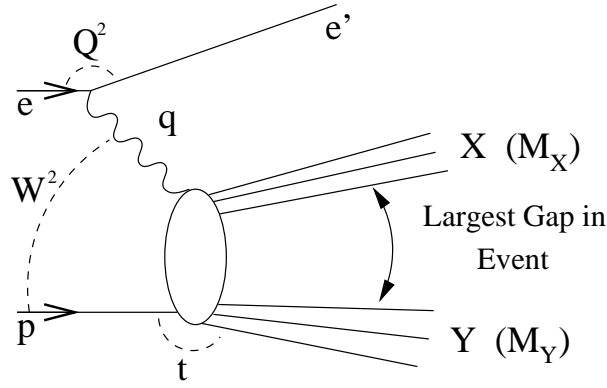


Figure 9: The diagram of the process with a rapidity gap between the system X and Y. The projectile nucleus is denoted here as p.

We shall consider in the following measurements of  $\frac{d^3\sigma(eA \rightarrow eXY)}{dx dQ^2 dx_{\mathcal{P}}}$ , from which the structure function  $F_{2,A}^{D(3)}(\beta, Q^2, x_{\mathcal{P}}) = \int F_{2,A}^{D(4)}(\beta, Q^2, x_{\mathcal{P}}, t) dt$  can be derived. The integration is over the range  $|t_{min}| < |t| < |t_{lim}|$  where  $t_{min}$  is a function of  $Q^2$ ,  $W^2$ ,  $\beta$  and the mass of the the system Y, and  $|t_{lim}|$  is specified by the requirement that all particles belonging to the system Y remain undetected. The structure function  $F_{2,A}^{D(3)}$  will thus be derived from

$$\frac{d^3\sigma_{eA \rightarrow eXY}}{dx dQ^2 dx_{\mathcal{P}}} = A \cdot \frac{4\pi\alpha^2}{xQ^4} \left\{ 1 - y + \frac{y^2}{2} \right\} F_{2,A}^{D(3)}(\beta, Q^2, x_{\mathcal{P}}). \quad (12)$$

The structure function  $F_{2,A}^{D(3)}(\beta, Q^2, x_{\mathcal{P}})$  can be measured at HERA using a sample of “rapidity gap” events i.e. events in which there is no hadronic energy flow over a large  $\eta$  interval. These events originate from coherent diffractive scattering ( $eA \rightarrow eA + X_{diff}$ ) and from incoherent diffractive scattering ( $eA \rightarrow e(A - N) + N + X_{diff}$ ).  $N$  denotes here the nucleons ejected from the incoming nucleus. The measurement of  $F_{2,A}^{D(3)}(\beta, Q^2, x_{\mathcal{P}})$  for several nuclei, separately for coherent and incoherent processes [4], will provide an important test of the quark parton interpretation of diffractive processes and a unique means to find out how universal is the concept of the pomeron.

We propose to measure the ratio of the structure functions

$$R_{A1,A2}(\beta, Q^2, x_{\mathcal{P}}) = F_{2,A1}^{D(3)}(\beta, Q^2, x_{\mathcal{P}}) / F_{2,A2}^{D(3)}(\beta, Q^2, x_{\mathcal{P}}), \quad (13)$$

where A1 and A2 denote the atomic numbers of the two nuclei. This ratio can be measured at HERA with a very high systematic accuracy. The statistical precision of such a measurement will be of the order of 5 %, if luminosities of  $10/A1$  and  $10/A2$   $\text{pb}^{-1}$  are collected for each nucleus. This is illustrated in Fig. 10 where we show, as an example,  $R_{A1,A2}$  at  $Q^2 = 12$   $\text{GeV}^2$  as a function of  $\beta$  and  $x_{\mathcal{P}}$ . In order to estimate the statistical precision of the measurement we have used the RAPGAP [38] Monte-Carlo and have assumed the event selection procedure of [36, 37]. We have not tried to model the nuclear dependence of the  $F_{2,A2}^{D(3)}(x, Q^2, x_{\mathcal{P}})$  resulting in the ratio shown in Fig. 10 to be equal 1.

Several distinct hypotheses concerning the deep inelastic structure of the diffractive processes can be verified (rejected) by measuring the  $R_{A1,A2}$ :

- universal (independent of the source) pomeron structure and an  $A$ -independent pomeron flux leading to

$$R_{A1,A2}(\beta, Q^2, x_{\mathcal{P}}) = 1; \quad (14)$$

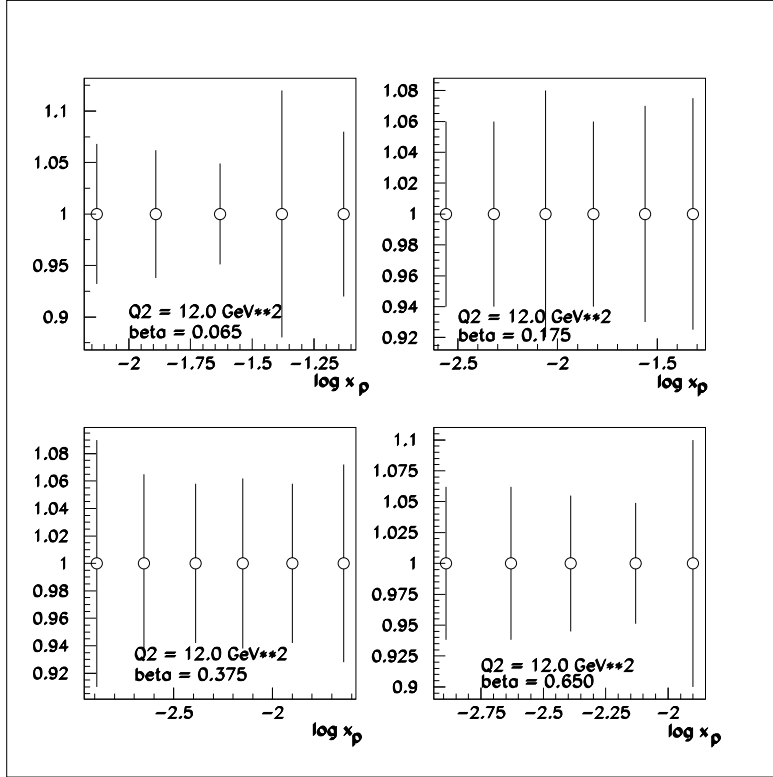


Figure 10: The ratio  $R_{A1,A2}(\beta, Q^2, x_P)$  plotted as a function of  $x_P$  for fixed values of  $\beta$  and  $Q^2$ . The error bars correspond to a luminosity of  $10/A1$  and  $10/A2$   $\text{pb}^{-1}$  for each nucleus.

- universal pomeron structure and an  $A$ -dependent pomeron flux leading to

$$R_{A1,A2}(\beta, Q^2, x_P) = f(A1, A2); \quad (15)$$

- $A$ -independent pomeron flux and a parent nucleus dependent pomeron structure. In a model of this type [39] the ratio  $R_{A1,A2}$  can be expressed using the nuclear structure functions  $F_{2,A}(x, Q^2)$  measured in inclusive electron nucleus scattering

$$R_{A1,A2}(\beta, Q^2, x_P) = F_{2,A1}(\beta \cdot x_P, Q^2) / F_{2,A2}(\beta \cdot x_P, Q^2). \quad (16)$$

### 2.4.3 Measurement of the $A$ -dependence of the Fraction of Rapidity Gap Events

One of the simplest measurements which could discriminate between the two pictures of pomeron formation proposed in [39, 40] and unresolved by the diffractive  $ep$  scattering data, is the measurement of the  $A$ -dependence of the fraction of the number of rapidity gap events with respect to the total number of deep inelastic scattering events:

$$R_{gap}(A1, A2) = \frac{N_{gap}(A1)/N_{tot}(A1)}{N_{gap}(A2)/N_{tot}(A2)}. \quad (17)$$

In the model of [39] the pomeron is replaced by multiple soft colour exchanges between the quark-antiquark pair into which the virtual photon has fluctuated and the target nucleus. In this model the ratio  $R_{gap}(A1, A2)$  is expected to be 1. This is in contrast to the prediction of the colour singlet exchange model [40] in which the ratio  $R_{gap}(A1, A2)$  can reach a value of 3 between nuclei with atomic numbers  $A1$  and  $A2$  differing by 200. In order to illustrate the

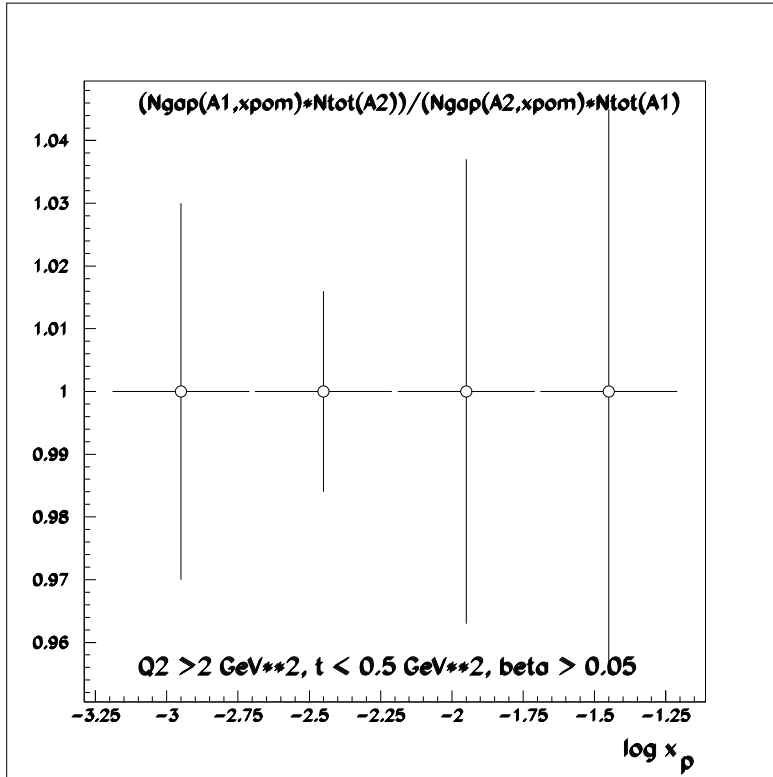


Figure 11: The integrated ratio  $R_{gap}(A1, A2)$  plotted as a function of  $x_P$ . The error bars correspond to a luminosity of  $1/A1$  and  $1/A2$   $\text{pb}^{-1}$  for each nucleus.

statistical precision of such a measurement we show in Fig. 11 the values of  $R_{gap}(A1, A2)$  and their statistical errors.

The statistical precision of  $R_{gap}(A1, A2)$  is dominated by the statistical precision of  $N_{gap}(A1)$  and  $N_{gap}(A2)$  and was determined with help of the RAPGAP [38] Monte Carlo by counting events generated within the kinematic domain defined by the following boundaries:  $Q^2 \geq 2$   $\text{GeV}^2$ ,  $|t| \leq 0.5$   $\text{GeV}^2$  and  $\beta \geq 0.05$ . The ratio shown in Fig. 11 was set to unity as we have not tried to model the nuclear dependence of the  $R_{gap}(A1, A2)$ . We observe that statistical precisions of  $\simeq 2$  % can be reached by collecting integrated luminosity of  $1/A$   $\text{pb}^{-1}$  for each nucleus. The systematic errors, as for the measurement of  $F_{2,A}^{D(3)}(\beta, Q^2, x_P)$  are expected to be smaller than the statistical errors if two nuclei are stored simultaneously at HERA. This measurement, even if carried out for two light nuclei, can easily rule out one of the two models of pomeron formation.

#### 2.4.4 Elastic Vector Meson Production

We present the accuracy expected for exclusive photoproduction of  $J/\psi$  mesons at  $Q^2 < 4$   $\text{GeV}^2$  ( $eA \rightarrow eAJ/\psi$ ) and exclusive production of  $\rho^0$  mesons at  $Q^2 > 4$   $\text{GeV}^2$  ( $eA \rightarrow eA\rho^0$ ).

As discussed in detail later, elastic (or exclusive) production of vector mesons in the reaction  $ep \rightarrow epV$ , where  $V$  is a vector meson ( $\rho^0$ ,  $\omega$ ,  $\phi$ ,  $J/\psi$ ...), is thought to be of a diffractive nature. Recent calculations (cf. e.g. [41, 42, 43, 44, 45]) indicate that the cross section for these processes may depend on the gluon momentum distribution  $\bar{x}G(\bar{x})$  probed at a value of  $\bar{x}$ , the fraction of the nucleon's momentum carried by the gluon,  $\bar{x} \simeq (Q^2 + m_V^2)/W^2$ , where  $m_V$  is the vector meson mass and  $W$  is the photon-nucleon centre-of-mass energy.

We have determined the statistical accuracy with which the ratios

$$R_V = \frac{1}{A^2} \frac{d\sigma^A/dt|_{t=0}}{d\sigma^D/dt|_{t=0}} \quad (18)$$

can be determined for  ${}^4\text{He}$ ,  ${}^{12}\text{C}$ ,  ${}^{32}\text{S}$  and  ${}^{208}\text{Pb}$ . Fig. 12 shows the results for  $J/\psi$  production.

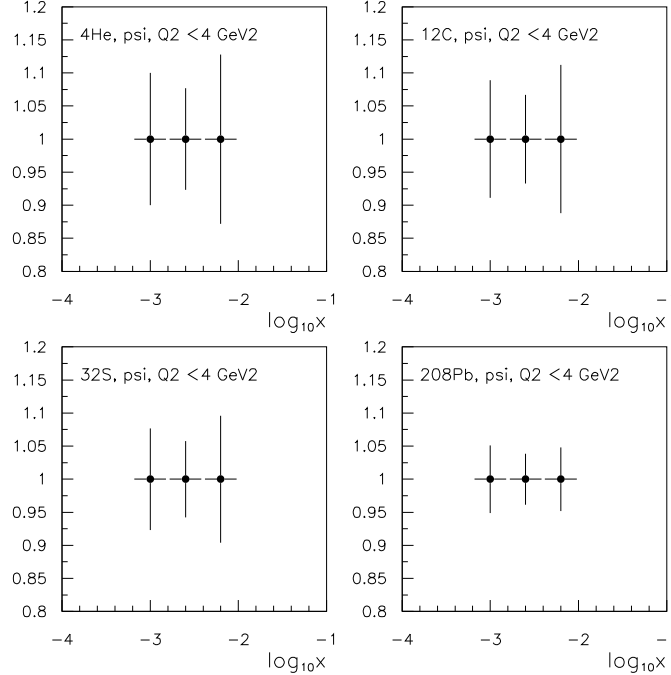


Figure 12: Expected statistical accuracy (vertical error bars) on the ratio  $R_V^{1/2}$  for elastic photoproduction ( $Q^2 < 4 \text{ GeV}^2$ ) of  $J/\psi$  mesons. In all cases a luminosity of  $1 \text{ pb}^{-1}/A$  for each nucleus was assumed. The horizontal bars indicate the size of the bins.

We used DIPSI [46], a Monte Carlo generator based on [41] that describes the available ZEUS data on  $J/\psi$  photoproduction. Events were generated in the range  $Q^2 < 4 \text{ GeV}^2$  and  $30 < W < 300 \text{ GeV}$ ; the  $J/\psi$  was assumed to decay into  $e^+e^-$  or  $\mu^+\mu^-$  pairs. Events in which the decay leptons were outside the coverage of the barrel and rear tracking detectors of H1 and ZEUS (approximately  $34^\circ < \vartheta < 164^\circ$ ) were rejected. A further reduction in the number of accepted events by a factor 0.2 was applied to account for efficiency and acceptance effects; this factor was taken to be independent of  $\bar{x}$ .

Only statistical uncertainties are shown. Possible sources of systematic uncertainties are the luminosity, the branching ratio, the global acceptance (including trigger and reconstruction efficiency, muon or electron identification etc.), the contamination from incoherent events, the feed-in from inelastic  $J/\psi$  production (à la photon-gluon fusion) and the feed-in from  $\psi'$  production. All the above contributions would largely cancel in a ratio for simultaneously stored nuclei, with the partial exception of the luminosity. In practice, for an integrated luminosity of  $1 \text{ pb}^{-1}$ , the statistical uncertainty is expected to dominate.

Fig. 13 shows the expected statistical uncertainty for  $\rho^0$  production at  $Q^2 > 4 \text{ GeV}^2$ . Here as well we used DIPSI, and the parameters were chosen so that the generator describes the ZEUS data [47]. Events were generated in the range  $4 < Q^2 < 100 \text{ GeV}^2$  and  $30 < W < 300 \text{ GeV}$ . The  $\rho^0$  was assumed to decay into  $\pi^+\pi^-$  pairs; pairs with masses between 0.3 and 1.4 GeV were considered. Events in which the decay pions were outside the coverage of the tracking detectors of H1 and ZEUS (approximately  $15^\circ < \vartheta < 164^\circ$ ) were rejected. A further reduction in the



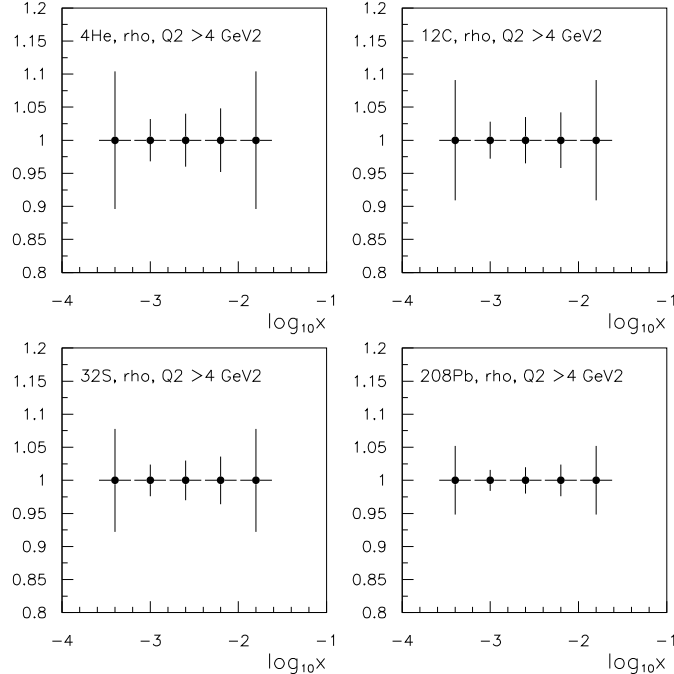


Figure 13: Expected statistical accuracy (vertical error bars) on the ratio  $R_V^{1/2}$  for elastic production ( $Q^2 > 4 \text{ GeV}^2$ ) of  $\rho$  mesons. In all cases a luminosity of  $1 \text{ pb}^{-1}/A$  for each nucleus was assumed. The horizontal bars indicate the size of the bins.

number of accepted events by a factor 0.6 was applied to account for efficiency and acceptance effects; this factor was independent of  $\bar{x}$ .

One can see from the figures that the accuracy of the measurements would be sufficient to discriminate between the colour transparency expectation of a ratio close to unity and the vector meson dominance expectation of the ratio  $R_V \approx A^{-2/3}$ ; cf. also the discussion in section 3.6.

## 2.5 Parton Propagation in Nuclei

This has been studied in various fixed target experiments in the past [48, 49]. It is investigated by measuring the final state hadrons in the deep inelastic scattering. Since there will be many more than one hadron per event in experiments at HERA the statistical errors are not expected to be a limitation and high accuracy should be possible. This subject is considered in more detail in section 3.7 and in [50].

## 2.6 Other Physics

In addition to the primary programme for nuclear beams in HERA outlined above there will be additional experiments which have not been explored in these studies. For example, there is physics interest in studying photoproduction from nuclear targets in the HERA energy range as well as sensitivity to physics beyond the standard model. Such sensitivity arises in  $e$ -nucleus collisions via coherent two photon interactions allowing production of positive C parity states which will be inhibited at LEP. This is discussed by Krawczyk and Levtchenko [51].

## 3 Theoretical Overview

### 3.1 Introduction

In this overview we describe those aspects of the phenomenology of QCD which lead to the nonlinear effects referred to earlier. These effects are thought to be related to the mechanisms which will eventually limit the growth of the nucleon structure function as  $x$  decreases at finite  $Q^2$ .

### 3.2 Space-time Picture of DIS off Nuclei at Small $x$

#### 3.2.1 The Rest Frame

In the rest frame of the target nucleus the life-time of a fluctuation is given by the formula

$$\tau = \frac{\beta}{m_N x_{Bj}}, \quad (19)$$

where  $\beta = Q^2/(Q^2 + M^2) < 1$ .  $M$  is the mass of the  $q\bar{q}$  system

$$M^2 = \frac{k_t^2 + m_q^2}{z(1-z)}, \quad (20)$$

where  $z$  is the light-cone momentum fraction,  $k_t$  the transverse momentum and  $m_q$  the mass of the quark. Perturbative QCD studies show that the most probable configurations are those for which  $M^2 \approx Q^2$ . In the case of transversely polarised photons both configurations with small  $k_t$  and highly asymmetric fractions  $z$  and configurations with comparable  $z$  and  $1-z$  contribute to the cross section. For the case of the longitudinal photons the asymmetric contribution is strongly suppressed.

In the language of noncovariant diagrams this corresponds to the virtual photon fluctuating into a quark-antiquark pair at a longitudinal distance  $l_c = \frac{\beta}{m_N x}$  from the nucleus which far exceeds the nuclear radius. The distance  $l_c$  is referred to as the ‘‘coherence length’’. The pair propagates essentially without transverse expansion until it reaches the target. QCD evolution leads to a logarithmic decrease of  $\beta$  with increasing  $Q^2$ . At HERA coherence lengths of up to 1000 fm are possible, so that the interaction of the  $q\bar{q}$  pair with nuclear matter can be studied in detail – notably its transparency to small size pairs - *colour transparency*.

At HERA new features of colour transparency should emerge: the incident small size  $q\bar{q}$  pair resolves small  $x$  gluon fields with virtualities  $\sim Q^2$ . If the transverse size of the  $q\bar{q}$  pair is  $r_t = b_q - b_{\bar{q}}$ , the cross section for interaction with a nucleon is [52]

$$\sigma_{q\bar{q},N}(E_{inc}) = \frac{\pi^2}{3} r_t^2 \alpha_s(Q^2) x g_N(x, Q^2), \quad (21)$$

where  $Q^2 \approx \frac{\lambda(x)}{r_t^2}$ ,  $\lambda(x \approx 10^{-3}) \approx 9$ ,  $x = \frac{Q^2}{2m_N E_{inc}}$ . Since the gluon density increases rapidly with decreasing  $x$ , even small size pairs may interact strongly, leading to some sort of *perturbative colour opacity* – the interaction of a small object with a large object with a cross section comparable to the geometric size of the larger object (Fig. 14).

Unitarity considerations for the scattering of a small size system [44] – i.e. the requirement that  $\sigma_{inel}(q\bar{q}, target) \leq \pi R_{target}^2$  – indicate that nonlinear effects (i.e. effects not accounted for by the standard evolution equations) should become significant at much larger values of  $x$  in  $eA$  scattering than in  $ep$  scattering.

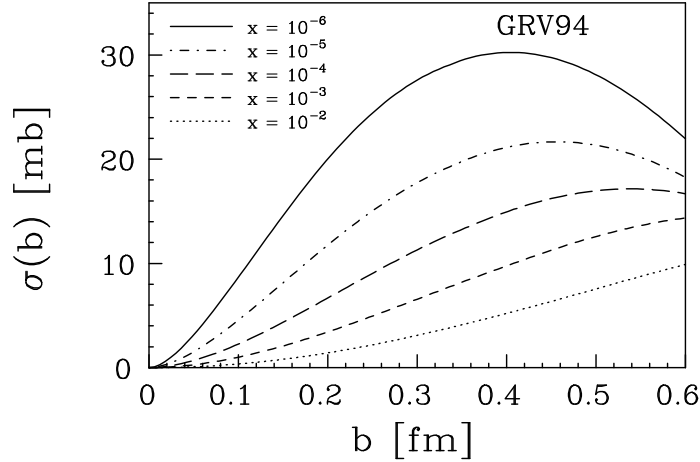


Figure 14: Colour-dipole cross section,  $\sigma_{q\bar{q}N}(x, b)$  of Eq. (21), as a function of the transverse size of the  $q\bar{q}$  pair for various values of  $x$  and for the GRV94 parametrization of the nucleon's gluon density.

### 3.2.2 The Breit Frame

In the Breit frame, small  $x$  partons in a nucleon are localized within a longitudinal distance  $\sim 1/xp_N$ , while the distance between two nucleons is  $\sim r_{NN}m_N/p_N$  ( $r_{NN}$  is the distance between nucleons in the rest frame and  $p_N$  is the nucleon momentum). Therefore partons with  $x < 1/(2m_N r_A)$ , where  $r_A \approx r_0 A^{1/3}$  fm is the nuclear radius and  $r_0 = 1.1$  fm cannot be localized to better than the whole nuclear longitudinal size. Hence low  $x$  partons emitted by different nucleons in a nucleus can overlap spatially and fuse, provided the density is high enough, leading to shadowing of the partonic distributions in bound nucleons with respect to the free nucleon ones and to nonlinear effects already at values of  $x \sim 10^{-4} \div 10^{-3}$ . For example, in the simplest model of nonlinear effects corresponding to the fan diagrams of Fig. 15, the additional contribution  $\delta g_A(x, Q^2)$  to  $g_A(x, Q^2)$  due to the nonlinear term in the equation for the  $Q^2, x$  evolution of the gluon density is [19]:

$$Q^2 \frac{\partial}{\partial Q^2} \frac{\delta x g_A(x, Q^2)}{A} = -\frac{81}{16} \frac{A^{1/3}}{Q^2 r_0^2} \alpha_s^2(Q^2) \int_x^1 \frac{du}{u} [u g_N(u, Q^2)]^2. \quad (22)$$

The analogous equation for the gluon density in the nucleon has a much smaller coefficient – approximately by a factor  $r_0^2/r_N^2 A^{1/3}$ , where  $r_N \sim 0.8$  fm is the nucleon radius. Once again one can see then that the  $x$ -range where nonlinear effects become significant differs for a heavy nucleus and for a nucleon by more than two orders of magnitude, assuming  $x g_N(x, Q^2) \propto x^n$  with  $n \sim -0.2$ .

Thus electron-nucleus collisions at HERA can be seen as efficient amplifiers of nonlinear QCD effects.

## 3.3 Theoretical Framework for Small $x$ Phenomena in $eA$ Collisions

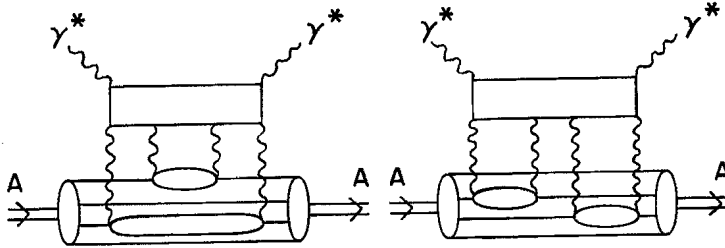


Figure 15: Typical fan diagrams leading to nonlinear evolution of  $g_A(x, Q^2)$ .

### 3.3.1 Perturbative and Nonperturbative Shadowing

At small  $x$  the DIS cross section per nucleon in a nucleus is smaller for a bound nucleon than for a free one, the so called shadowing phenomenon. Shadowing is determined by a combination of non-perturbative and perturbative effects. In the DGLAP evolution equations one can express shadowing at large  $Q^2$  through the shadowing at the normalization point  $Q_0^2$ . This type of shadowing is connected to the soft physics. It can be visualized e.g. in the aligned jet model of Bjorken [2], extended to account for QCD evolution effects [53]. A virtual photon converts to a  $q\bar{q}$  pair with small transverse momenta (large transverse size) which interacts with the nucleus with a hadronic cross section, leading to shadowing. The effective small phase volume of these configurations ( $\propto \frac{\lambda}{Q^2}$ ) leads to Bjorken scaling and it is due to colour transparency [53].

At large  $Q^2$ , these  $q\bar{q}$  pairs evolve into systems with gluons, leading to a shift of shadowing to smaller  $x$ , which is equivalent to the standard  $Q^2$  evolution of parton distributions. These  $q\bar{q}$  pairs, which interact with the target nonperturbatively, seem to be responsible for most of the shadowing at intermediate  $Q^2$  and  $x \sim 10^{-2}$  which has been studied at fixed target energies. This mechanism of shadowing is effective for  $\sigma_T$  only since for  $\sigma_L$  the aligned jet contribution is strongly suppressed. For  $\sigma_L$  (as well as for the production of heavy quarks) one is more sensitive to the shadowing due to the interaction of small size  $q\bar{q}$  pairs with the nuclear gluon field which can be shadowed.

At smaller  $x$  the situation may change rather dramatically because, as the recent HERA data indicate, already for  $Q^2 \sim 1.5 \text{ GeV}^2$  at  $x \sim 10^{-4}$  perturbative contributions to  $F_{2p}(x, Q^2)$  appear to become important, leading to a rapid increase of the structure functions with decreasing  $x$ . Hence contributions of various perturbative mechanisms which may generate shadowing for configurations of a size smaller than the hadronic size may become important. Perturbative QCD may be applicable to those small size pairs. Typical contributions involve diagrams of the eikonal type, various enhanced diagrams, etc. (Fig. 15,16).

### 3.3.2 Shadowing and Diffraction

In practically all models it is assumed that nuclei are built of nucleons. So the condition that the matrix element  $\langle A|T[J_\mu(y)J_\nu(0)]|A \rangle$  involves only nucleonic initial and final states is implemented<sup>1</sup>. Under these natural assumptions one is essentially not sensitive to any details

<sup>1</sup> The condition that nuclei are built of nucleons is not so obvious in the fast frame picture. However it is implemented in most of the models [19, 54].

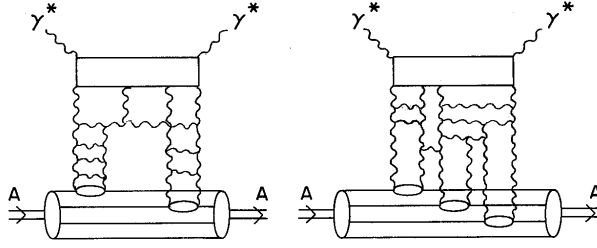


Figure 16: Examples of typical perturbative QCD diagrams contributing to nuclear shadowing.

of the nuclear structure, such as short-range correlations etc.

In the case of scattering off the deuteron and light nuclei the same diagrams contribute to the cross section for diffraction in  $ep$  scattering and the cross section for shadowing – hence similar nonlinear phenomena like those described by eq.(22) are involved in each case. For example for the deuteron [1]:

$$\sigma_{shad} = \frac{\sigma_{tot}(eD) - 2\sigma_{tot}(eN)}{\sigma(eN)} = \frac{\frac{d\sigma_{diff}(ep)}{dt}|_{t=0}}{\sigma_{tot}(ep)} \frac{1}{8\pi R_D^2} R, \quad (23)$$

where  $R = \frac{(1-\lambda^2)}{(1+\lambda^2)}$ ,  $\lambda = ReA/ImA \approx \frac{\pi}{2} \frac{\partial \ln A}{\partial \ln s}$  for the amplitude  $A$  of  $\gamma^*p$  scattering and  $R_D$  is the deuteron radius. For small  $x$ ,  $\lambda$  may be as large as 0.5, leading to  $R \sim 0.5$  especially for the case of the longitudinal cross section. So already for light nuclei the study of the total cross sections of scattering from nuclei would allow *to establish a fundamental connection between the two seemingly unrelated phenomena of diffraction at small  $t$  in  $ep$  scattering and nuclear shadowing*. With the increase of  $A$  more complicated nonlinear interactions with several nucleons become important, see e.g. Fig. 16b.

Nuclear shadowing for the total cross sections has a simple physical meaning - it corresponds to a reduction of cross section due to screening of one nucleon by another (as well as by several nucleons for  $A > 2$ ). If one treats the deuteron as a two nucleon system it is possible to apply the Abramovskii, Gribov, Kancheli (AGK) cutting rules [55] to elucidate **the connection between nuclear shadowing, diffraction and fluctuations of multiplicity**. One observes that the simultaneous interaction of the  $\gamma^*$  with the two nucleons of the deuteron modifies not only the total cross section but also the composition of the produced final states. It increases the cross section for diffractive scattering off the deuteron due to diffractive scattering off both nucleons by  $\delta\sigma_{diff} = \sigma_{shad}$ . At the same time the probability to interact inelastically with one nucleon only is reduced since the second nucleon screens the first one:  $\delta\sigma_{single} = -4\sigma_{shad}$ . In addition, a new process emerges in the case of the deuteron which was absent in the case of the free nucleon - *simultaneous* inelastic interaction with both nucleons which leads to a factor of two larger multiplicity densities for rapidities away from the current fragmentation region:  $\sigma_{double} = 2\sigma_{shad}$ . Altogether these contributions constitute  $-\sigma_{shad}$ , the amount by which the total cross section is reduced <sup>2</sup>.

<sup>2</sup>For simplicity we give here relations for the case of purely imaginary  $\gamma^*N$  amplitude  $\frac{ReA}{ImA} = 0$ .

To summarize, *there is a deep connection between the phenomena of diffraction observed at HERA in ep scattering and nuclear shadowing as well as the A-dependence of diffraction and the distribution of the multiplicities in DIS.*

It follows from the above discussion that it is possible to get information about the dynamics of nuclear shadowing and hence about nonlinear effects by studying several **key DIS phenomena** such as: nuclear shadowing for inclusive cross sections  $F_2^A, \frac{\sigma_L}{\sigma_T}, F_2^{Acharm}$ ; the cross section for nuclear diffraction; the multiplicity distribution for particle production in the central rapidity range; diffractive production of vector mesons. The advantage of the latter process is that one gets a rather direct access to the interaction of a small colour dipole with matter. It is in a sense an exclusive analogue of  $\sigma_L$  which is easier to measure.

### 3.4 The A-Dependence of Parton Distributions at Small $x$

As discussed above, the nucleus serves as an amplifier for nonlinear phenomena expected in QCD at small  $x$ . The simplest example of such effects is given by equation (22) where the nonlinear term is proportional to the square of the nucleon gluon density. If shadowing were absent the parton densities per unit transverse area would be enhanced by a factor  $A^{1/3}$  as compared to the free nucleon case. Hence even just an upper limit on the parton densities based on unitarity – that the cross section for the inelastic interaction of a small dipole with a nucleus may not exceed  $\sigma_{inel} = \pi R_A^2$  – leads to the expectation of nonlinear phenomena – shadowing of an observable magnitude – already at  $x \sim 10^{-3} \div 10^{-4}$  [44].

Hence, from detailed studies of the A-dependence of the parton densities it would be possible both to check the dominance of the two-nucleon screening mechanism for  $x \sim 10^{-2}$  [56, 57] and to extract information about the coherent interaction of the virtual photon with three (four) nucleons at  $x \leq 10^{-3}$ .

For  $x \geq 10^{-2}$  for any nucleus and for all  $x$  for light nuclei, the main contribution to shadowing is given by the interaction with two nucleons of the target. Hence in this regime there is a relatively simple connection with the diffraction of a virtual photon off a proton – which is the simplest nonlinear effect in the perturbative domain in QCD. For smaller  $x$  and heavy nuclei, when essential longitudinal distances become comparable and ultimately exceed the diameter of the nucleus, several nucleons at the same impact parameter contribute to the screening. It is worth emphasizing that these multi-vacuum exchange processes cannot be singled out unambiguously using a nucleon target. The relevant QCD diagrams for the total cross section of  $\gamma^*A$  interaction are rather similar to higher-order nonlinear diagrams for the proton target – except that in the nuclear case one has to impose the condition that couplings to the individual nucleons are colour singlets, see e.g. Fig. 15,16.

In a sense, the studies of nuclear shadowing at small  $x$  and large  $Q^2$  can be considered as a simpler model of nonlinear effects which occur in the case of a nucleon target. In the latter case it is not easy to relate the coupling of say two vacuum exchanges (or a ladder with 4 gluons in the  $t$ -channel) with a nucleon to the coupling of one vacuum exchange with a nucleon. In fact the region of  $10^{-3} \geq x \geq 10^{-4}$  may be optimal in this respect since nonlinearities for the nucleon case are still small though nonlinearities for the nuclear case are already quite substantial. It is worth emphasizing that experience of the studies of the total hadron-nucleus scattering indicates that interaction with bound nucleons for the total cross sections can well be

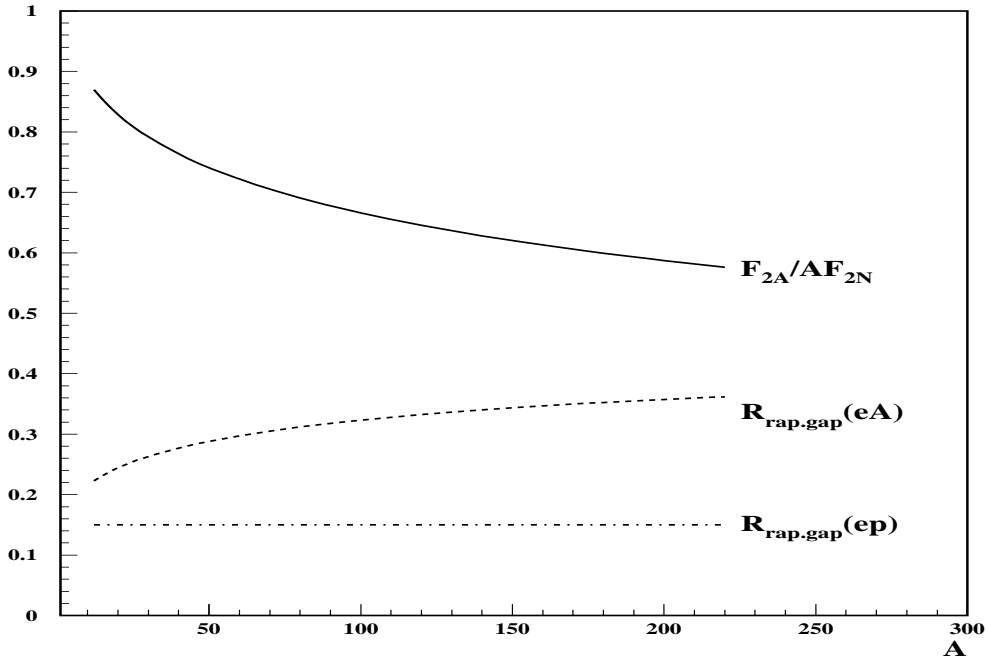


Figure 17:  $A$ -dependence of nuclear shadowing and probability of rapidity gap events in the colour screening model of shadowing; dot-dashed curve assumes  $A$ -independent probability of rapidity gap events.

approximated by the interactions with free nucleons (for a recent analysis see [58]). Therefore *nuclear structure effects do not obscure the interpretation of nuclear shadowing effects*.

Using current information from HERA on diffractive production in  $ep$  scattering it is straightforward to estimate the amount of nuclear shadowing at small  $x$  taking into account interactions with 3 or more nucleons using the eikonal approximation with an effective cross section determined from diffractive data, see eq.(24) below. The result of the calculation [40] is shown in Fig. 17 for  $Re/Im = 0$ ; for  $A \geq 12$  it weakly depends on the value of  $Re/Im$ . Since the data on diffraction indicate that the fraction of diffractive events in DIS weakly depends on  $x, Q^2$  these considerations show that significant shadowing effects should be present for  $F_2^A(x, Q^2)$  in the wide small  $x$  range of HERA. Note that the shadowing effect in DIS is expected to be much smaller than for the case of real photon scattering since the effective cross section for interaction of the hadron component of quasi-real photon at HERA is a factor of  $\sim 3$  larger than for a highly virtual photon (we use here the HERA data on diffraction for real photons [59]).

Since the interaction of the octet colour dipole  $gg$  is a factor of  $9/4$  stronger than for the  $q\bar{q}$  dipole, nonlinear effects are expected to be more important for gluons. So gluon shadowing would provide even more direct access to nonlinear phenomena. Note that in this case there is no simple relation of shadowing with diffraction in  $\gamma^* + p$  DIS, so any information about gluon shadowing would be complementary to the information from  $ep$  DIS. There are very few data on the gluon distribution in nuclei. Among them, the enhancement of the gluon distribution at  $x \sim 0.1$  indicated by the inelastic  $J/\psi$  production data [25]. Also the analysis [60] of the scaling violation for the ratio  $F_2^{Sn}/F_2^C$  [11] under the assumption that higher twist effects are not important in the  $Q^2, x$  range of the data allows to extract information about the  $A$ -

dependence of gluon distributions, indicating some nuclear shadowing for  $G_A$  for  $x \leq 0.01$  and an enhancement at  $x \sim 0.1$ , see Figure in [60]<sup>3</sup>. Theoretical expectations for gluon shadowing discussed in the literature are quite different – from a larger effect than for  $F_2^A$  [63], to an effect comparable to that of quarks [62, 61, 64, 65] to substantially smaller shadowing [66]; see also contributed papers to these proceedings.

Comparison of different determinations of shadowing of gluons and measurements of the scaling violation for the  $F_2^A/F_2^D$  ratios will allow to determine the range of applicability of the DGLAP evolution equations and hence provide unique clues to the role of nonlinear effects.

It is worth emphasizing also that knowledge of parton distributions in bound nucleons at these values of  $x$  will be crucial also for studies in heavy-ion physics at the LHC and RHIC.

### 3.4.1 BFKL Pomeron

One can envision several strategies for the study of the BFKL Pomeron in DIS. The main requirement is to enhance the contribution of scattering of small transverse size configurations in the ladder. It is natural to expect that screening for these configurations would be minimal. Hence for heavy nuclei the contribution of the BFKL Pomeron can be enhanced.

1. A procedure can be envisioned to study the  $A$ -dependence of  $F_2^A(x, Q^2)$  at small  $x$  to extract the term in the structure functions  $\propto A$  and then study its  $x$  dependence. Based on the above argument A.Mueller has suggested [67] that the  $x$  dependence of this term (linear in  $A$ ) would be closer to BFKL type behaviour.
2. One promising direction to look for the BFKL pomeron is the Mueller-Navalet process of producing two high  $p_t$  jets with large a rapidity difference [68] to suppress the contribution from small transverse momenta (large transverse distances) in the ladder. In the case of a nuclear target large distance contributions would be screened out to a large extent.
3. Another possibility is the production of  $\rho$  mesons at large  $|t|$  in inelastic diffraction. To enhance the contribution of the BFKL Pomeron it is desirable to increase the contribution of small configurations in the  $\rho$  meson, i.e. quark-antiquark pairs with small transverse separation. Large size configurations can be filtered out by exploiting the fact that they are absorbed on the nucleus surface. Once again extracting the term in the cross section  $\propto A$  would allow to enhance the contribution of the BFKL Pomeron.

## 3.5 Diffraction off Nuclei

### 3.5.1 Introduction

Diffraction studies have been defined as one of the primary goals of nuclear beams in HERA. Such processes can be interpreted using two complementary languages depending on whether the rest frame of the nucleon or the Breit frame are used:

- Scattering of electrons on colourless components of the proton [36, 37]. Such scattering may be identified, for the very low  $x$  events dominated by diffraction, with the interaction with

---

<sup>3</sup>The shadowing for gluons should be accompanied by a significant enhancement at larger  $x$  since the total momentum fraction carried by gluons in nuclei is not suppressed and is probably slightly enhanced [61].



the vacuum  $t$ -channel exchange which is often referred to as the Pomeron,  $\mathbb{P}$ . This object is not necessarily the same as the Pomeron of the Gribov-Regge high-energy soft interactions (see report of the diffractive group). Deep inelastic electron scattering leading to the presence of a rapidity gap can thus be considered as probing the internal parton structure of the  $\mathbb{P}$  originating from the proton.

One of the questions of primordial importance which may be addressed within the future electron-nucleus scattering program at HERA is then “how universal is the internal structure of the Pomeron?” or, more precisely: “Is the internal structure of the Pomeron originating from various hadronic sources (protons, neutrons, nuclei) the same?”. We shall show below how nuclei may help in answering these questions.

- The diffractive interaction of different hadronic components of the virtual photon with the target via vacuum exchange. Diffraction predominantly selects the  $\gamma^*$  components which interact with sufficiently large cross sections such as large transverse size  $q\bar{q}$ ,  $q\bar{q}g$  colour dipoles. Therefore the study of diffraction plays a very important role in determining the relative importance of small and large size configurations and addressing the question whether small white objects interact weakly or not. Indeed if the interaction with a target becomes sufficiently strong at small impact parameters the cross section for diffraction (which includes both elastic scattering and inelastic diffractive dissociation) would reach the black body limit of 50% of the total cross section.

### 3.5.2 Theoretical Expectations

Diffraction off a nucleon (including dissociation of the nucleon) constitutes about 15-20% of the deep inelastic events. Therefore the interaction is definitely far from being close to the scattering off a black body. Even this number came a surprise in view of the large  $Q^2$  value involved. Using the generalized optical theorem as formulated by Miettinen and Pumplin, one can estimate the effective total cross section for the interaction of the hadronic components of the  $\gamma^*$  as

$$\sigma_{eff} = 16\pi \frac{\left. \frac{d\sigma_{diff}^{\gamma^*+p \rightarrow X+p}}{dt} \right|_{t=0}}{\sigma_{tot}(\gamma^*N)} \approx 12 \div 15 \text{mb}. \quad (24)$$

This cross section is significantly smaller than the  $\rho N$  cross section which at the HERA energies can be estimated to be close to 40 mb using the vector dominance model and the Landshoff-Donnachie fit [69]:

$$\sigma_{tot}^{\rho N}(s) = \sigma_{tot}^{\rho N}(s_0) \left( \frac{s}{s_0} \right)^n, \quad (25)$$

where  $n \approx 0.08$ ,  $s_0 = 200 \text{ GeV}^2$ ,  $\sigma_{tot}^{\rho N}(s_0) = 25 \text{ mb}$ . However it is sufficiently large to result in a substantial cross section of diffraction for small  $x$  – it can reach 30-40% for large  $A$  (Fig. 17)[40]. For large  $A$  the coherent diffraction dominates when the incoming wave is sufficiently absorbed at small impact parameters which, by virtue of Babinet’s principle, corresponds to scattering beyond the nucleus. In such processes the nucleus remains intact and the average momentum transfer is very small ( $\langle t \rangle \propto A^{-2/3}$ ).

One expects that hadronic configurations interacting with different strength contribute to diffraction (cf. Fig. 14). The parameter  $\sigma_{eff}$  characterizes just the average strength of this

interaction, while the distribution over the strengths is expected to be quite broad. The study of diffraction off nuclei allows to separate contributions to diffraction of large and small size configurations due to **the filtering phenomenon**: with the increase of  $A$  the relative contribution of more weakly interacting (smaller size) configurations should increase since they are less shadowed, leading to a relative enhancement of the colour transparent subprocesses.

Examples of promising processes are:

- Diffractive production of charm. The  $A$ -dependence of this process would be interesting already at low  $Q^2$  since the essential transverse distances are, naively, of the order of  $1/m_c$ , where  $m_c$  is the charm quark mass. Since the cross section for the interaction of a colour dipole of such size is small for  $x \sim 10^{-2}$ , the cross section for diffractive charm production at these values of  $x$  is small and practically not shadowed, leading to a cross section  $\propto A^{4/3}$ . At the same time the  $c\bar{c} - N$  cross section increases rapidly with decreasing  $x$  (increase of energy) for fixed  $Q^2$ . Therefore at HERA energies diffractive charm production in  $ep$  collisions may become a substantial part of the total diffractive cross section. At this point one expects the emergence of shadowing in diffractive charm production in  $eA$  collisions, leading to slowing down of the  $A$ -dependence of diffractive charm production as compared with the  $A$  dependence at  $x \sim 10^{-2}$ .

One can go one step further and study the  $A$ -dependence of  $p_t$  distributions for diffractive charm production. Smaller size components will be less absorbed and so their relative contribution may increase with  $A$ .

- Diffractive production of two high  $p_t$  jets.

Selection of large  $p_t$  jets enhances the contribution of diffraction of small size configurations. Hence, one expects broader  $p_t$  distributions in the case of nuclear targets (smaller jet alignment) with nontrivial dependences on  $W$  and  $Q^2$ . For example, if we fix the  $p_t$  of the jets, the  $A$ -dependence of dijet production should become weaker with increasing energy reflecting the increase of the absorption (which can be studied this way). If on the other hand we fix  $W$  and consider the  $A$ -dependence as a function of  $p_t$ , a stronger  $A$ -dependence is expected. Effectively, this would be another way to approach colour transparency via filtering out of the soft components.

To summarize, a study of inclusive diffraction will give better insights into the structure of the Pomeron. The interplay of soft and hard contributions will lead to a breakdown of factorization for the structure function of the Pomeron. Stated differently, the check of the degree of “universality” of the Pomeron – i.e. whether the “nuclear” Pomeron is different from the Pomeron observed in  $ep$  diffraction – will provide a very sensitive test of QCD dynamics.

An important aspect of the diffractive studies is the colour transparency phenomenon. In view of its special interest we will discuss this separately below.

### 3.5.3 Multiplicity Fluctuations

As we explained in section 3.3.2 diffraction off nuclei and nuclear shadowing are closely related to the simultaneous inelastic interactions of the virtual photon with several nucleons. Such interactions produce events with large multiplicity densities in the central rapidity range, leading to a much broader distribution over multiplicities in  $eA$  collisions than in the  $ep$  case. Study

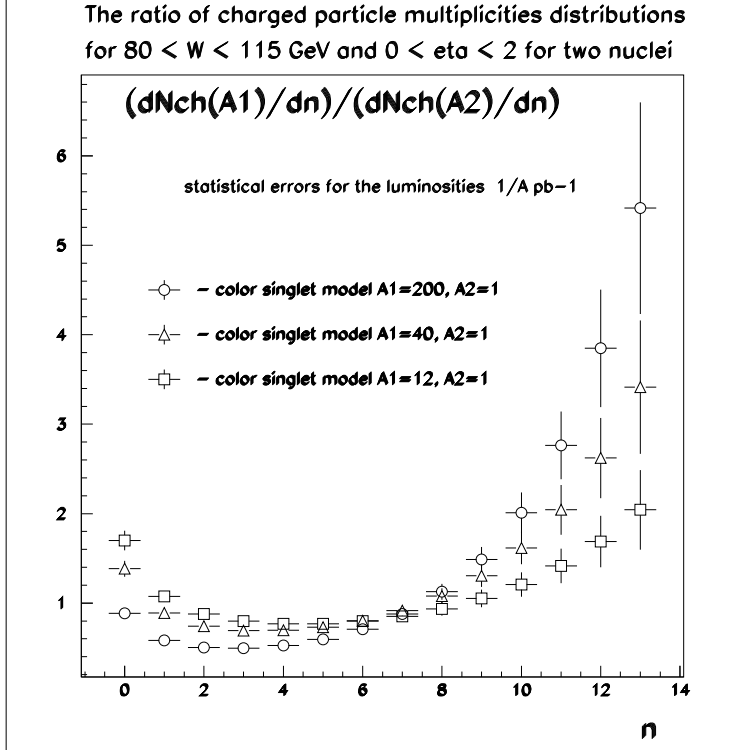


Figure 18:  $A$ -dependence of distribution over multiplicity calculated in the colour singlet model for a luminosity of  $1 \text{ pb}^{-1}$ .

of this effect will provide information complementary to that obtained from nuclear shadowing about the structure of the vacuum exchange at small  $x$ . Interesting phenomena to look for may be:

1. Local fluctuations of multiplicity in the central rapidity region, e.g. the observation of a broader distribution of the number of particles per unit rapidity,  $n(\Delta\eta)$ , than in  $ep$  scattering [40], see Fig. 18.
2. Long range rapidity fluctuations – i.e. positive correlation of the increase of multiplicity in one rapidity interval with the increase of multiplicity several units away.
3. Correlation of the central multiplicity with the multiplicity of neutrons in the neutron detector (most effective for heavy nuclei).

### 3.6 Colour Transparency Phenomena

An important property of QCD is that small objects are expected to interact with hadrons with small cross section [70]. This implies that in the processes dominated by the scattering/production of hadrons in “point-like” (small size) configurations (PLC) when embedded in the nuclei, the projectile or the outgoing hadron essentially does not interact with the nuclear environment [71, 72]. In the limit of colour transparency one expects for an incoherent cross section a linear dependence on  $A$ , for example

$$\frac{d\sigma(e + A \rightarrow e + p + (A - 1)^*)}{dQ^2} = Z \frac{d\sigma(e + p \rightarrow e + p)}{dQ^2}, \quad (26)$$

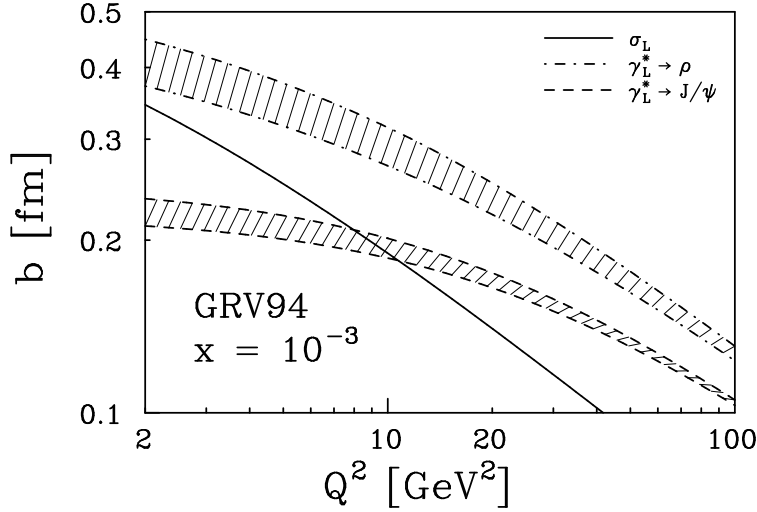


Figure 19: Average transverse size of the  $q\bar{q}$  components effective in  $\mathcal{A}_{\gamma_L^* N \rightarrow VN}$  for  $\rho$ - and  $J/\psi$ -meson production and  $\sigma_L$ . The probed  $Q^2$  scale is inversely proportional to  $b^2$ .

while for coherent processes at  $t = 0$  one expects

$$\frac{d\sigma(\gamma^* + A \rightarrow X + A)}{dt} = A^2 \frac{d\sigma(\gamma^* + N \rightarrow X + N)}{dt}. \quad (27)$$

No decisive experimental tests of this property of QCD were performed so far since in most of the current experiments the energies were not sufficiently high to prevent expansion of the produced small system. The high-energy E665 experiment [73] at FNAL has found some evidence for colour transparency in the  $\rho$  meson production off nuclei. However, the data have low statistics, cover a small  $x, Q^2$  range and cannot reliably separate events without hadron production.

A quantitative formulation of colour transparency for high-energy processes can be based on eq.(21). For the case of nuclear targets it implies that for a small enough colour dipole, the cross section of its interaction with nuclei is proportional to  $A$  up to the gluon shadowing factor. As a result the colour transparency prediction for 2 jet and vector meson diffractive production is [74, 42]<sup>4</sup>:

$$\frac{\frac{d\sigma}{dt}(\gamma^* A \rightarrow 2jets + A)|_{t=0}}{\frac{d\sigma}{dt}(\gamma^* N \rightarrow 2jets + N)|_{t=0}} = \frac{\frac{d\sigma}{dt}(\gamma^* A \rightarrow VA)|_{t=0}}{\frac{d\sigma}{dt}(\gamma^* N \rightarrow VN)|_{t=0}} = \left[ \frac{F_A^L(x, Q^2)}{F_N^L(x, Q^2)} \right]^2 = \frac{G_A^2(x, Q^2)}{G_N^2(x, Q^2)}. \quad (28)$$

Gluon shadowing constitutes a rather small effect for  $x \sim 10^{-2}$  (see earlier discussion). For smaller  $x$  it increases but it is in any case much smaller than the screening effect expected in the case of lack of colour transparency if the produced system interacts with cross section comparable to  $\sigma_{\rho N} \sim 30\text{-}40$  mb. For such values of  $\sigma$  one expects the cross section to behave as  $\propto A^{4/3}$  for  $t = 0$  which would be possible to test using diffractive production by quasi-real photons.

#### *Coherent diffractive $\rho, J/\psi$ -meson production*

<sup>4</sup>In writing eq.(28) we neglect the difference of  $Q^2$  scales for different processes which is reflected in a different dependence of the essential transverse size of the  $q\bar{q}$  state on the process (see Fig. 19). For a discussion of the appropriate scale for dijet production see [75].

The most straightforward test of colour transparency can be made using coherent production of  $\rho$  or  $J/\psi$ -mesons at small  $t$  using nuclei with  $A \geq 12$ . The  $p_t$  resolution of the current detectors is good enough to single out the diffractive peak which is concentrated at  $p_t \leq 0.1$  GeV. In the higher  $x$  end of the range which could be studied at HERA for vector meson production,  $x \sim 10^{-2}$ , one expects at large  $Q^2$  nearly complete colour transparency since gluon shadowing effects are rather small and decrease rapidly with increase of  $Q^2$ , while the transverse separation,  $b$ , between  $q$  and  $\bar{q}$  is of the order of 0.4 fm for  $Q^2 \sim 10$  GeV<sup>2</sup> and further decreases with increase of  $Q^2$  (Fig. 19 [44]). Study of coherent  $J/\psi$  meson production would allow to probe colour transparency for propagation of even smaller dipoles since  $\langle b_{c\bar{c}}(Q^2 = 0) \rangle \sim 0.2$  fm.

On the other hand as discussed earlier at the smallest values of  $x$  of the HERA range, screening effects should start to play a role even at large  $Q^2$  so a gradual disappearance of colour transparency is expected – the emergence of colour opacity. Noticeable screening is expected already on the basis of unitarity constraints. Qualitatively one may expect that the rise of the cross section for vector meson production with increasing energy at fixed  $Q^2$  will slow down at significantly lower energies than for the case of the  $\gamma^* + p$  reaction. Currently theoretical calculations of vector meson production by transversely polarised photons are difficult because the nonperturbative large distance contribution is not as strongly suppressed in this case as in the longitudinal case. If contribution of pairs with large transverse size is indeed important for  $\sigma_T$ , it would be filtered out with increasing  $A$  leading to larger values of  $\sigma_L/\sigma_T$  for large  $A$ .

Let us enumerate several other effects of Colour Transparency (CT) in diffractive production.

1. Production of excited vector meson states  $\rho', \phi'$ .

In the CT limit, QCD predicts a universal  $A$ -dependence of the yields of the lowest mass and excited states (this includes the effect of gluon shadowing in eq.(28)). This is highly nontrivial since the sizes of the excited states are much larger, so one might expect larger absorption. On the other hand, for lower  $Q^2$  average transverse distances,  $b$ , are not small. At these distances the wave functions of ground and excited states differ. So in this  $Q^2$  range the relative yields of various mesons may depend on  $A$ .

2. Production of high  $p_t$  dijets.

The uncertainty relation indicates that coherent production of dijets with large  $p_t$ , carrying all the momentum of the diffractively produced system is dominated by distances  $r_t \propto \frac{1}{p_t}$ . Hence filtering out of soft jets is expected, leading to a broadening of the  $p_t$  and thrust distributions. At the same time the study of the  $A$ -dependence of low  $p_t$  jets would allow to address the question of colour opacity. Another feature to look for would be the distribution over the electron-two jet plane angle as suggested in [76].

3. Coherent diffractive production at  $-t \geq 0.1$  GeV<sup>2</sup> for  $A = 2, 4$ .

An important question here is the possibility to observe the “disappearance” of colour transparency for  $\rho$ -meson production and the emergence of “colour opacity” – due to nonlinear screening effects at  $x \sim 10^{-4}$ . Manifestations of CT would be the increase of the differential cross section  $\frac{d\sigma}{dt}$  below the diffractive minimum ( $|t_{min}(^4He)| \approx 0.2$  GeV<sup>2</sup>) and suppression of the cross section in the region of the secondary maximum. A gradual disappearance of CT in this region with increasing energy would appear as a very fast increase with energy of the secondary maximum of the  $t$  distribution. Remarkably, in this region the cross section for the process is proportional to  $[G_N(x, Q^2)]^4$ , where  $G_N$  is the

gluon density in the nucleon [77, 78]. The present beam optics would allow measurements of quasielastic processes with  ${}^4\text{He}$  in the region of the secondary maximum ( $|t({}^4\text{He})| \approx 0.4 \text{ GeV}^2$ ). For a luminosity of  $10 \text{ pb}^{-1}$  it would be possible to measure the  $\rho$ -meson production cross section up to  $Q^2 \sim 10 \text{ GeV}^2$ .

#### 4. $A$ -dependence of rapidity gaps between jets in photoproduction.

Recently photoproduction events which have two or more jets have been observed in the range  $135 < W_{\gamma p} < 280 \text{ GeV}$  with the ZEUS detector at HERA [79]. A fraction of the events has little hadronic activity between the jets. The fraction of these events,  $f(\Delta\eta)$ , reaches a constant value of about 0.1 for large pseudorapidity intervals  $\Delta\eta \geq 3$ . The observed number of events with a gap is larger than that expected on the basis of multiplicity fluctuations assuming the exchange of a colour singlet. This value is rather close to estimates in perturbative QCD [80, 81, 82] neglecting absorptive effects due to interactions of spectator partons. It is much larger than the values reported by D0 [83] and CDF [84]. Small effects of absorption are by no means trivial in view of the large interaction cross section for many components of the hadronic wave function of the real photon. They may indicate that colour transparency is at work here as the ZEUS trigger may select point-like configurations in the photon wave function [85]. To check this idea it would be natural to study the  $A$ -dependence of rapidity gap survival. It is demonstrated in [85] that this probability strongly depends on the effective cross section of the interaction of the photon with the quark-gluon configurations involved in producing rapidity gap events. One would be sensitive to cross sections as small as  $\sim 5 \text{ mb}$ .

## 3.7 Parton Propagation in Nuclear Matter

### 3.7.1 Introduction

Measurements of final state hadrons allow to investigate the effects of partons propagating through nuclear matter. In the present section we discuss some of these possibilities. The discussion is restricted to *incoherent* phenomena (coherent nuclear interactions were discussed in previous sections).

There are essentially two types of measurements which can be useful: (a) energy loss of high-energy particles and (b) increase of their transverse momentum, both studied as a function of the nuclear number  $A$  and/or number of nucleons emitted from the target nucleus. They are sensitive to different aspects of the interactions. Energy loss reflects the properties of inelastic collisions: the value of the inelastic parton-nucleon cross section and of the inelasticity. The increase of transverse momentum and emission of the nucleons from the target can be induced by elastic as well as by inelastic collisions and thus can provide information on both.

At this point we emphasize the importance of the measurement of the distribution of the nucleons (protons and neutrons) emitted from the target nucleus during or after the interaction. Such measurements give direct access to the number of secondary interactions inside the target [86], as was already realized (and used) in numerous emulsion experiments where protons with momenta  $250 \leq p_N \leq 700 \text{ MeV}/c$  were measured [87]. Related information can be inferred from the measurement of the production of soft neutrons ( $E_n \leq 10 \text{ MeV}$ ) which was studied recently by the E665 collaboration [88]. Measurements of the emitted nucleons and of their energy spectrum should thus be considered a high priority. They allow to improve greatly the

analysis of the data in three respects: (a) by studies of the distribution of nucleons themselves one obtains information of the strength of the secondary interactions and - more essentially- on the fluctuations which are expected to be large and would otherwise hamper the interpretation of the data; (b) By studying the interactions as a function of the number of the emitted nucleons one can obtain not only a larger lever arm in terms of the number of secondary interactions but also, at a *fixed* nuclear number, a clean sample, free of possible biases related to the use of different targets; (c) a really exciting possibility is to develop a trigger for events with a large number of emitted nucleons (or highly reduced charge of the nuclear remnant). This would allow to study in detail the rare events with particularly strong secondary interactions. Further quantitative studies (both theoretical and experimental) of this problem are necessary to clarify the relation between the emitted nucleons and number of secondary interactions. Some work on these lines was already presented during this workshop [89, 4, 90]. The detection of such nucleons at HERA will be simpler than in fixed target experiments since they will be boosted by the motion of the target nucleus [4].

As we discussed previously there should be a substantial difference between the nuclear effects observed in the region of “finite”  $x$  ( $x$  greater than, say, 0.05) and the region of very small  $x$  ( $x$  smaller than, say, 0.001). The reason is the different nature of the photon-nucleon interactions in these two regions caused by the difference in life times of the relevant photon fluctuations into a  $q\bar{q}$  pair.

One sees from eq.( 19) that at finite  $x$  the life time of a fluctuation is rather short (smaller than 2 fm). This has two consequences: (a) the interaction of the photon must take place inside one of the nucleons of the target (nuclear coherence suppressed) and (b) the high-energy part of the interacting photon fluctuation can be well approximated by a simple “bare” quark. This can be seen as follows. The time necessary to produce a high-energy gluon from a quark is given by

$$\tau_g = \frac{2E_g}{q_t^2} \quad (29)$$

where  $E_g$  is the gluon energy and  $q_t$  its transverse momentum (with respect to the quark). From the obvious condition  $\tau_g < \tau$  we then obtain

$$E_g < \frac{\beta k_t^2}{2m_N x}. \quad (30)$$

We conclude that at finite  $x$  there is simply no time to produce the energetic gluon cloud.

For DIS nuclear collisions this picture implies that after the first interaction of the virtual photon the nucleus is penetrated by one bare quark (following approximately the direction of the virtual photon). Alternatively one can consider the process of production of two high  $p_t$  jets in *photon-gluon fusion*. In this case one studies propagation through the nucleus of a colour octet state. Thus the observed nuclear effects measure interactions of a *bare* parton (or a system of *bare* partons) in nuclear matter.

The situation is rather different in the region of small  $x$ . In this case there is enough time for the  $q\bar{q}$  system coupled to the virtual photon to “dress” itself into a cloud of energetic gluons and  $q\bar{q}$  pairs (in the limit  $x_{Bj} \rightarrow 0$  the condition (30) is not restrictive). Consequently, the system traversing the nucleus is a complex multiparton system resembling in some respects an “ordinary” hadron. The observed nuclear effects measure interactions of this multiparton system (*dressed* quark or  $q\bar{q}$  dipole) in nuclear matter. It should thus not be surprising that the expectations for the region of small  $x$  are rather different from those at finite  $x$ .

### 3.7.2 Current Experimental Situation

Two major manifestations of the interaction of a parton propagating through the nuclear medium which were studied experimentally so far are the parton energy loss and the broadening of its transverse momentum distribution.

The measurements of the leading hadron spectrum in deep inelastic lepton-nucleus scattering have the biggest sensitivity to the energy loss. Measurements at incident energies below 50-100 GeV find a depletion of the leading particle spectrum which may be interpreted as due to the energy loss. At higher energies the effect nearly disappears [49], indicating that energy losses for partons propagating through nuclear matter are definitely smaller than  $\Delta E/dz \leq 1$  GeV/fm. This is in agreement with the observed low multiplicity of low energy neutrons in  $\mu Pb$  interactions at high energies [88], which is consistent with knockout of one nucleon from lead [90]. This makes it impossible to address directly the question of energy losses at high energies.

The phenomenological situation with transverse momentum broadening is somewhat confusing at the moment. The  $\mu$ -pair production experiments [91] which measure the broadening of the *incident* quark find rather small broadening:  $\Delta p_t^2 \sim 0.1 \text{ GeV}^2$  for the distance,  $L \sim 5$  fm. At the same time the transverse momentum broadening for the jets produced by *outgoing* partons in photon-nucleus interactions seems to be much larger [92]. Theoretically this difference is not understood [93].

### 3.7.3 Perturbative QCD Expectations for Finite $x$

All estimates of nuclear effects in this region of  $x$  accept that the interaction of a *bare* quark in nuclear matter is dominated by colour-exchange processes which lead to break-up of the “wounded” nucleon in the target but do not slow down significantly the energetic quark. This is based on the argument that the quark in question can only emit gluons satisfying the condition  $\tau_g < \Delta l$  where  $\Delta l$  is the distance between the subsequent collisions. From eq.(29) we deduce that the energy loss in one secondary collision is limited by

$$\Delta E < 2q_t^2 \Delta l, \quad (31)$$

i.e., by a value which is independent of the energy of the quark. Consequently, a high energy quark can lose only a small fraction of its energy. A precise evaluation of the energy loss in a collision with one target nucleon is not possible at the present stage of the theory.

However recently a significant progress was obtained in the analysis of the propagation of a virtual parton through the nuclear medium [3]. It was demonstrated that the Landau-Pomeranchuk-Migdal effect in QCD is qualitatively different from the case of QED. It was argued that for sufficiently large distances,  $L$ , traversed by a parton the process is dominated by perturbative QCD though the momentum transfers in the individual collisions are small.

A simple relation was found between the  $p_t$  broadening and the energy loss

$$-\frac{dE}{dL} = \frac{\alpha_s N_c}{8} \Delta p_t^2(L), \quad (32)$$

which corresponds to substantially smaller energy losses than those implied by the inequality in eq.(31).



Probably the most striking prediction is the quadratic dependence of the energy loss on the traversed distance,  $L$ , as compared to the nonperturbative models where it is approximately proportional to  $L$ . Numerically the authors find for a quark

$$-\Delta E \simeq 2\text{GeV} \left( \frac{L}{10 \text{ fm}} \right)^2, \quad (33)$$

neglecting the  $x$  dependence of the nucleon gluon density (and a factor of  $\sim 2$  larger energy loss for gluons). If this effect is included the  $L$ -dependence is even steeper. The numerical coefficient is estimated here from the information on the nucleon gluon densities and consistent with eq.( 32) if one uses experimental data on  $p_t$  broadening of the  $\mu$ -pair spectrum [91]. Alternatively, if one uses the  $p_t$  information from  $\gamma A$  data a much larger energy loss is predicted. However even in this case the expected energy loss is too small to be observed *directly* in DIS at collider energies.

The energy loss occurs (for realistic nuclei) via the emission of one or two gluons with energies  $\sim \Delta E$ . So it would be the best to look for the energy loss effects by studying the production of hadrons in the nucleus fragmentation region. Quadratic dependence on  $L$  will be manifest in the  $A$ -dependence of the number of knocked out nucleons, as well as in the fluctuations of the number of emitted soft protons and neutrons in the case of heavy nuclei. Current HERA detectors have good acceptance for such nucleons.

Broadening of the transverse momentum spectrum may be more easy to access. The transverse momentum of a parton increases as a result of multiple collisions. Since the momentum transfers in the subsequent collisions are independent, the increase of the (average) transverse momentum squared is proportional to  $L$  and hence to the number of secondary collisions. One expects for the quark

$$\Delta p_t^2 \simeq 0.2\text{GeV}^2 \frac{L}{10\text{fm}}, \quad (34)$$

while for gluons broadening is about a factor of 2 larger.

A word of caution is necessary here. For distances typical even for heavy nuclei the average momentum transfer is rather small so application of perturbative QCD may be difficult to justify. Also it is not clear whether it is safe to interpolate from fixed target energies to collider energies assuming that the momentum transfer in individual collisions is energy independent.

To study these effects at HERA in a clean way one needs to consider processes dominated by relatively large  $x \geq 0.1$ . They include processes of dijet production similar to those studied at FNAL [92]. An advantage of HERA is that it would be possible to use information about the decay of the nucleus to check the correlation between transverse momentum broadening and the number of struck nucleons.

### 3.7.4 Parton Propagation at Small $x$

This region is more relevant for HERA but, unfortunately, theoretical estimates are difficult and uncertain because the system traversing the nucleus is fairly complicated. Hence its interaction with nuclear matter not easy to evaluate. Perturbative QCD leads to the simple prediction that at large  $Q^2$  and large incident energies, due to QCD factorization, the spectrum of leading hadrons [72] is given by,

$$\frac{1}{\sigma^{\gamma^*A}(x, Q^2)} \frac{d\sigma^{\gamma^*+A \rightarrow h+X}(x, Q^2, z)}{dz} = f(z, \ln Q^2), \quad (35)$$

which does not depend on  $A$ . (Energy losses we discussed above do not change the  $z$  spectrum in this limit). However, it is far from clear if perturbative methods are applicable at all - even at large  $Q^2$  [94]. The incoming system can experience several soft interactions with the nucleons of the target nucleus. However, the AGK technique which can be used to relate nuclear shadowing with the  $A$  dependence of diffraction and the fluctuations of hadron production in the central region, does not allow any predictions for the  $A$  dependence of the spectrum of leading hadrons in the current fragmentation region since these effects depend on the details of the virtual photon wave function. In view of these difficulties it is not possible to give unbiased quantitative predictions and we restrict ourselves to a discussion of qualitative expectations and possible interpretations of the future measurements.

As we have already mentioned, at small  $x$  the virtual photon fluctuates into a  $q\bar{q}$  pair a long time before it enters the nucleus. This has several consequences. First, it opens the possibility of *coherent* phenomena in which the nucleus participates as a whole which were discussed in a previous section. They should be carefully separated from the incoherent interactions we are concerned with. Second, there is enough time for this fluctuation to emit a large number of gluons and new  $q\bar{q}$  pairs *before* it enters the nucleus. The cross-section of such a “dressed” fluctuation is generally fairly large, leading to substantial “shadowing” effects, as already discussed. Finally, the system produced in the first collision is by no means a single bare quark but rather a multiparton conglomerate - result of a quark-gluon cascade of length equal to the available rapidity, i.e. very long at small values of  $x$ . Studies of interactions in nuclear matter provide an opportunity to obtain information about this object.

The cascade origin of the system travelling through the nucleus implies strong correlations between partons. Consequently, large fluctuations are expected in its physical properties and thus also in the observable nuclear effects. For example, the cross section for secondary interactions is expected to vary widely from event to event. This variation may or may not be correlated with the fluctuations of the parton multiplicity and energy distributions. For a clean interpretation of the results it is therefore crucial to obtain information on the number of secondary interactions inside the nucleus which is the most important parameter determining the strength of the interaction. Fortunately, as we have already explained, this information is accessible through measurements of the distribution of nucleons (protons and neutrons) emitted by the colliding nucleus. They seem thus crucial for the success of this investigation.

The distribution of the number of collisions gives straightforward information on the fluctuations of the cross section for secondary interactions inside the nucleus. Its change as  $Q^2$  increases from 0 to the deep inelastic region should give information on the extent to which the structure of parton bound states (i.e. hadrons) differs from that of the “dressed”  $q\bar{q}$  pair.

Similar remarks apply to measurements of the energy loss (which measures the energy distribution inside the parton system in question). Correlation between the observed energy loss and the number of collisions gives information on clustering phenomena inside the parton system. It will be interesting to look for possible effects of constituent quarks at low  $Q^2$  and to see when they disappear as  $Q^2$  increases. Fig. 20 illustrates the possibility of such an investigation. It shows the ratio of the total energy loss of the incident virtual photon in the nucleus to that in collision with one nucleon, assuming that the photon fluctuates into  $K$  constituents which interact independently (losing energy) with the target. One sees that the curves corresponding to different values of  $K$  are substantially different. This seems to give a chance to see possible effects of constituent quarks ( $K = 2$ ) at low  $Q^2$  which should gradually disappear ( $K \rightarrow \infty$ ) as  $Q^2$  increases. It should be remembered, however, that variations in

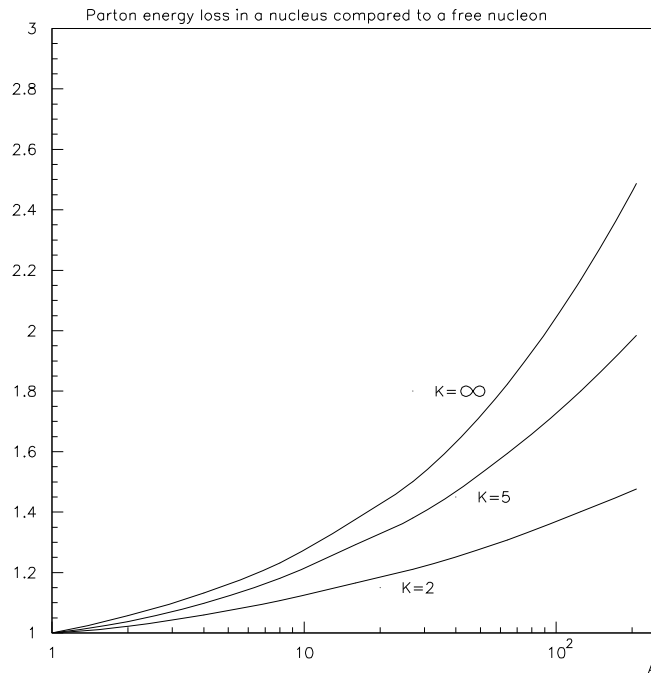


Figure 20: Energy loss of the incident virtual photon in nuclei assuming that the photon fluctuates into  $K$  constituents interacting independently in nuclear matter with an interaction cross section of 20 mb.

the cross-section of the photon fluctuation in question will smear out this clean effect. It is therefore necessary to rely on an independent estimate of the number of collisions as we already emphasized at the beginning of this section. In this case the ratio in question is given by

$$\frac{\Delta E_A}{\Delta E_1} = K(1 - (1 - 1/K)^N) \quad (36)$$

( $N$  is the number of collisions) and one can easily see that this is indeed a much better way to analyze the data, particularly at high  $N$ .

It should be noted at this point that, in contrast to the situation at finite  $x$ , in the present case the energy loss is expected to be a finite fraction of total available energy, as explained above. Consequently, there seem to be no particular difficulties in this measurement.

To summarize, one expects a dramatic increase of the energy loss in nuclear matter when one goes from finite to small values of  $x$ . If confirmed by future data this should allow to study details of the parton structure of the QCD cascade. Investigation of the transition region of  $x \approx 0.01$  is also of great interest. HERA is very well suited for this task.

### 3.8 Connection to Heavy-ion Collisions at High Energies

The interplay between the physics which can be studied in high-energy  $eA$  collisions at HERA and that to be studied in the heavy ion physics was discussed at the dedicated workshop “Nuclei at HERA and Heavy Ion Physics” which was held at Brookhaven National Laboratory in 1995. It was concluded that the measurements of  $eA$  collisions at HERA can provide crucial

information necessary for unambiguous interpretation of the heavy ion collisions at RHIC and LHC for establishing whether a quark-gluon plasma is formed in these collisions.

Three major links are

- *Nuclear gluon shadowing*

One needs  $xg_A(x, Q^2)$  for  $x \sim 10^{-2}$ ,  $Q^2 \sim 1 - 10\text{GeV}^2$  and  $x \sim 10^{-3}$ ,  $Q^2 \sim 10\text{GeV}^2$  to fix the initial conditions at RHIC and LHC respectively. This is especially important for the LHC since mini-jet production determines the initial conditions for  $\sqrt{s} \geq 100\text{GeV}$ . The bulk of the particles produced at central rapidities in  $AA$  collisions at the LHC is expected to be generated due to this mechanism [95]. Currently uncertainties in nuclear shadowing transform into at least a factor 2-4 differences in the final transverse energy flow [96].

- *Jet quenching*

Recent QCD studies [97] have demonstrated that the medium induced energy losses and  $p_t$  broadening of a high energy parton traversing a hot QCD medium are much larger than in the case of a cold medium. This provides a unique new set of global probes of the properties of the state formed during  $AA$  collisions [96]. To interpret unambiguously this effect it is necessary both to measure the nuclear gluon shadowing and to study the parton propagation in cold matter in DIS to confirm that the energy losses ( $p_t$ -broadening) remain small at energies comparable to those to be studied at RHIC and LHC.

- *Testing of soft dynamics of interactions with nuclei*

Study of  $eA$  interactions at HERA in **the same energy range** as that to be studied in  $pA$  and  $AA$  collisions at RHIC ( $\sqrt{s} \sim 200\text{ GeV}$ ) will provide a unique testing ground for the modern models of interactions with nuclei which aim at describing on the same footing  $ep, eA, pp, pA, AA$  collisions [89]. It would allow to be established whether or not the same dynamics determines hadroproduction in  $eA$  collisions and in central  $AA$  collisions.

## 4 Acknowledgements

We thank all our colleagues in working group 8 for their invaluable assistance and for numerous discussions. AB acknowledges support by the KBN grant No 2 P03B 083 08 and by a PECO grant from the EEC Programme ‘‘Human Capital and Mobility’’, Network ‘‘Physics at High Energy Colliders’’, Contract No ERBICIPDCT940613. MS thanks the U.S. Department of Energy for financial support under grant number DE-FG02-93ER-40771.

## References

- [1] V. N. Gribov, Sov. Phys. JETP **30** 709 (1969).
- [2] J. D. Bjorken in Proceedings of the International Symposium on Electron and Photon Interactions at High Energies, p. 281–297, Cornell (1971).
- [3] R. Baier, Yu.L. Dokshitzer, A.H. Mueller, S. Peigné and D. Schiff, hep-ph 9608322 and these proceedings.

- [4] J. Chwastowski and M.W. Krasny, “What can we gain by detecting nuclear fragments in electron-nucleus collisions at HERA?”, these proceedings.
- [5] K. Kurek, “QED Radiative Processes in Electron-Heavy Ion Collisions at HERA”, these proceedings.
- [6] I. Akushevich and H. Spiesberger, “Radiative Corrections to Deep Inelastic Scattering on Heavy Nuclei at HERA”, these proceedings.
- [7] NMC, M. Arneodo et al., Nucl. Phys. **B 441** (1995) 3.
- [8] NMC, M. Arneodo et al., Nucl. Phys. **B 441** (1995) 12.
- [9] E665, M.R. Adams et al., Z. Phys. **C 67** (1995) 403.
- [10] NMC, M. Arneodo et al., “The  $A$  dependence of the nuclear structure function ratios”, submitted to Nucl. Phys. B.
- [11] NMC, M. Arneodo et al., “The  $Q^2$  dependence of the structure function ratio  $F_2^{Sn}/F_2^C$  and the difference  $R^{Sn} - R^C$  in deep inelastic muon scattering”, submitted to Nucl. Phys. B.
- [12] EMC, J.J. Aubert et al., Phys. Lett. **B 123** (1983) 275.
- [13] EMC, J. Ashman et al., Phys. Lett. **B 202** (1988) 603 and Z. Phys. **C 57** (1993) 211.
- [14] EMC, M. Arneodo et al., Phys Lett **B 211** (1988) 493 and Nucl. Phys. **B 333** (1990) 1.
- [15] SLAC, A. Bodek et al., Phys. Rev. Lett. **50** (1983) 1431, *ibid.* **51** (1983) 534 and R. G. Arnold et al., *ibid.* **52** (1984) 727.
- [16] BCDMS, G. Bari et al., Phys. Lett. **B 163** (1985) 282 and A.C. Benvenuti et al., *ibid.* **B 189** (1987) 483.
- [17] For a review of the experimental and theoretical situation of nuclear effects in DIS see e.g. L.L. Frankfurt and M.I. Strikman, Phys. Rep. **160** (1988) 235; T. Sloan, G. Smadja and R. Voss, Phys. Rep. **162** (1988) 45; R.J.M. Covolan and E. Predazzi, in “Problems of Fundamental Modern Physics”, Editors R. Cherubini, P. Dalpiaz and B. Minetti, World Scientific, Singapore (1991) p. 85; M. Arneodo, Phys. Rep. **240** (1994) 301.
- [18] J. Kwiecinski, A.D. Martin and P.J. Sutton, Phys. Rev. **D52** (1995).
- [19] A.H. Mueller and J-W. Qiu, Nucl. Phys. **B268** (1986) 427.
- [20] A.D. Martin, R.G. Roberts and W.J. Stirling RAL Report TR 96-037 and Int. J. of Mod Phys **A10** (1995) 2885.
- [21] H1, S. Aid et al., Nucl. Phys. **B449** (1995) 3.
- [22] D. Graudenz, CERN-TH-95-121, April 1995. Talk given at Workshop on Deep Inelastic Scattering and QCD (DIS 95), Paris, France, 24-28 April 1995.
- [23] EMC, J.J. Aubert et al., Nucl. Phys. **B 213** (1983) 1 and J. Ashman et al., Z. Phys. **C 56** (1992) 21.

- [24] NMC, D. Allasia et al., Phys. Lett. **B 258** (1991) 493.
- [25] NMC, P. Amaudruz et al., Nucl. Phys. **B 371** (1992) 553.
- [26] H1, S. Aid et al., Nucl. Phys. **B 472** (1996) 3.
- [27] ZEUS, M. Derrick et al., paper pa-02 47 submitted to the XXVIII International Conference on High Energy Physics Warsaw, July 25-31, 1996.
- [28] H1, S. Aid et al., paper pa-02 73 submitted to the XXVIII International Conference on High Energy Physics Warsaw, July 25-31, 1996.
- [29] T. Weiler, Phys. Rev. Lett. **44** (1980) 304.
- [30] E.L. Berger and D. Jones, Phys. Rev. **D 23** (1981) 1521.
- [31] R. Baier and R. Rückl, Nucl. Phys. **B 201** (1981).
- [32] A.D. Martin, C.-K. Ng and W.J. Stirling, Phys. Lett. **B 191** (1987) 200.
- [33] M. Krämer et al., Phys. Lett. **B 348** (1995) 657 and Nucl. Phys. **B 459** (1996) 3.
- [34] ZEUS, M. Derrick et al. Phys. Lett. **B315** (1993) 481.
- [35] H1, T. Ahmed et al. Nucl. Phys. **B429** (1994) 477.
- [36] H1, T. Ahmed et al., Phys. Lett. **B348** (1995) 681.
- [37] ZEUS, M. Derrick et al. Z. Phys. **C68** (1995) 569.
- [38] H. Jung, “Hard Diffractive Scattering in High Energy  $ep$  Collisions and the Monte Carlo Generator RAPGAP”, DESY preprint DESY 93–182 (1993), to appear in Comput. Phys. Commun.
- [39] W. Buchmuller and A. Hebecker, Phys. Lett. **B355** (1995) 573.
- [40] L. Frankfurt and M. Strikman, Phys. Lett. **B382** (1996) 6.
- [41] M.G. Ryskin, Z. Phys. **C 57** (1993) 89.
- [42] S.J. Brodsky, L. Frankfurt, J.F. Gunion, A.H. Mueller and M. Strikman, Phys. Rev. **D50** (1994) 3134.
- [43] J. Nemchik et al., Phys. Lett. **B341** (1994) 228.
- [44] L. Frankfurt, W. Koepf and M. Strikman, Tel-Aviv University preprint TAUP-2290-95 (1995); Phys. Rev. **D54** (1996) 3194.
- [45] M.G. Ryskin et al., “Diffractive  $J/\psi$  photoproduction as a probe of the gluon density”, Rutherford Lab. preprint RAL-TR-95-065, hep-ph/9511228 (1995).
- [46] M. Arneodo, L. Lamberti and M. G. Ryskin, DESY report DESY 96-149, to appear in Comp. Phys. Comm.
- [47] ZEUS Collab., M. Derrick et al., Phys. Lett. **B 356** (1995) 601.

- [48] EMC, J. Ashman et al., Z.Phys. **C52** (1991) 1.
- [49] E665, M.R.Adams et al., Z.Phys. **C61** (1994) 179.
- [50] N.Pavel, these proceedings.
- [51] M. Krawczyk and B. B. Levtchenko, these proceedings.
- [52] B. Blättel, G. Baym, L.L. Frankfurt and M. Strikman, Phys. Rev. Lett. **71** (1993) 896.
- [53] L. L. Frankfurt and M. Strikman, Phys. Rep. **160** (1988) 235.
- [54] L.M Lerran and R.Venugopalan, Phys.Rev. **D50** (1994) 225.
- [55] V.Abramovskii, V. N. Gribov and O. V. Kancheli, Sov. J. Nucl. Phys. **18**, 308 (1974).
- [56] L. L. Frankfurt and M. I. Strikman, Nucl. Phys. **B316** (1989) 340.
- [57] B.Z.Kopeliovich and B.Povh, Phys.Lett. **B367** (1996) 329 and contribution to these proceedings.
- [58] B.K. Jennings and G.A. Miller Phys. Rev. **C49** (1994) 2637.
- [59] H1, S.Aid et al., Z. Phys. **C69** (1995) 27.
- [60] T.Gousset and H.J. Pirner, Phys.Lett.**B375** (1996) 354 and contribution to these proceedings.
- [61] L.Frankfurt, M.Strikman and S. Liuti, Phys. Rev. Lett. **65** (1990) 1725.
- [62] J.W.Qiu Nucl.Phys. **B291** (1987) 746.
- [63] L. Frankfurt, M. Strikman and S. Liuti, Proceedings of the Conference on Particles and Nuclei XIII, Perugia, Italy (1993) page 342, edited by A. Pascolini (published by World Scientific).
- [64] K.J. Eskola, Nucl.Phys.**B400** (1993) 240.
- [65] K.J. Eskola, Jian-wei Qiu, Xin-Nian Wang, Phys.Rev.Lett.**72** (1994) 36.
- [66] N.N.Nikolaev and V.G.Zakharov, Z.Phys. **C49** (1991) 607.
- [67] A.H.Mueller, In the proceedings of the BNL workshop on Nuclei at HERA and Heavy Ion Physics, BNL-62634 (1995).
- [68] A.H.Mueller and H.Navelet, Nucl.Phys. **B282** (1987) 727.
- [69] A.Donnachie and P.Landshoff, Phys.Lett **B296** (1992) 227.
- [70] F. E. Low, Phys. Rev. **D12** (1975) 163.
- [71] S.J. Brodsky in Proceedings of the Thirteenth International Symposium on Multiparticle Dynamics, ed. W. Kittel, W. Metzger and A. Stergiou (World Scientific, Singapore, 1982) page 963.

- [72] A.H. Mueller in Proceedings of the Seventeenth Rencontre de Moriond, Moriond, 1982 ed. J. Tran Thanh Van (Editions Frontieres, Gif-sur-Yvette, France, 1982) Vol. I, page 13.
- [73] E665, M.R. Adams et al., Phys.Rev.Lett. **74** (1995) 1525.
- [74] L. Frankfurt, G.A. Miller and M. Strikman, Phys. Lett. **B304** (1993) 1.
- [75] J.Bartels, H.Lotter and M. Wusthoff, Phys.Lett. **B379** (1996) 239.
- [76] J.Bartels, C.Ewerz, H.Lotter, M.Musthoff, DESY 96-085.
- [77] H.Abramowicz, L.Frankfurt and M.Strikman, DESY-95-047; SLAC Summer Inst.1994:539-574.
- [78] L. Frankfurt, W.Koepf, M.Sargsyan, M.Strikman, contribution to these proceedings.
- [79] ZEUS, M.Derrick et al., Phys.Lett. **B369** (1996) 55.
- [80] J.D.Bjorken, Phys.Rev. **D47** (1992) 101.
- [81] A.H.Mueller and W.-K.Tang, Phys.Lett. **B284** (1992) 123.
- [82] V.Del Duca and W.-K.Tang, Phys.Lett. **B312** (1993) 225.
- [83] D0, S.Abachi et al., Phys.Rev.Lett. **72** (1994) 2332; FERMILAB-PUB-95-302-E(1995).
- [84] CDF, S.Abe et al, Phys.Rev.Lett. **74** (1995) 85.
- [85] L.Frankfurt and M.Strikman, contribution to these proceedings.
- [86] B.Andersson, I.Otterlund and E.Stenlund, Phys.Lett. **B73** (1978) 343.  
J.Babecki and G.Nowak, Acta Phys. Polonica **B9** (1978) 401.
- [87] see e.g. J.Babecki et al., Acta Phys.Polonica **B9** (1978) 495.
- [88] E665, M.R.Adams et al Phys.Rev.Lett. **74** (1995)5198.
- [89] K. Geiger, Contribution to these proceedings; J.Ellis, K. Geiger and H. Kowalski, to be published in Phys.Rev.D, e-Print Archive: hep-ph/9605425.
- [90] M.Strikman, M.Tverskoy, M.Zhalov, these proceedings.
- [91] D.M. Alde et al., Phys.Rev.Lett. **66** (1991) 2285 and references therein.
- [92] T. Fields and M.D. Corcoran, in the EPS Conference proceedings, Marseille, France, July 22-28, 1993; Phys.Rev.Lett. **70**,143,1993;  
R.C. Moore, et al., Phys.Lett. **B244** (1990) 347 ;  
M.D. Corcoran, et al., Phys.Lett. **B259** (1991) 209.
- [93] M. Luo, J. Qiu and G. Sterman, Phys.Rev.**D49**(1994) 4493.
- [94] J.Bjorken, SLAC-PUB-7096, January 1996.
- [95] X-N.Wang and M.Gyulassy, Phys.Rev.Lett. **68** (1992) 1480.
- [96] M.Gyulassy, Proc. 'Nuclei at HERA and Heavy Ion Physics', BNL-62634, 1995.
- [97] R. Baier, Yu.L. Dokshitzer, A.H. Mueller, S. Peigné and D. Schiff hep-ph 9607355.